In presenting the dissertation as a partial fulfillment of the requirements for an advanced degree from the Georgia Institute of Technology, I agree that the Library of the Institute shall make it available for inspection and circulation in accordance with its regulations governing materials of this type. I agree that permission to copy from, or to publish from, this dissertation may be granted by the professor under whose direction it was written, or, in his absence, by the Dean of the Graduate Division when such copying or publication is solely for scholarly purposes and does not involve potential financial gain. It is understood that any copying from, or publication of, this dissertation which involves potential financial gain will not be allowed without written permission.

7/25/68

EXPERIMENTAL AND ANALYTICAL INVESTIGATION OF AN IMPACT CONFIGURATION FLUIDIC AMPLIFIER

A THESIS

Presented to

The Faculty of the Graduate Division

by

Charles Willard Minch

In Partial Fulfillment

of the Requirements for the Degree

Master of Science in Mechanical Engineering

Georgia Institute of Technology

January 1970

EXPERIMENTAL AND ANALYTICAL INVESTIGATION

OF AN IMPACT CONFIGURATION FLUIDIC AMPLIFIER

Approved:

Chairman

Date approved by Chairman: January 26, 1970

ACKNOWLEDGMENTS

I wish to thank my Thesis Advisor, Dr. P. V. Desai, and Dr. S. L. Dickerson for their originating the thesis topic. I also wish to thank the thesis committee, Dr. S. L. Dickerson and Dr. B. C. Spradlin, for their time and suggestions. Mr thanks go also to Mr. R. A. Whisnant for his suggesting the method of fabricating the fluidic device. My appreciation is extended to Mrs. Louise K. Barge for her kind assistance in typing the manuscript and to the technicians of the School of Mechanical Engineering for their assistance in constructing the test system.

I am indebted to Dr. S. P. Kezios, Director of the School of Mechanical Engineering, for financial assistance in the form of The Whirlpool Fellowship and a graduate teaching assistantship. I am grateful to my wife for her assistance and encouragement through these academic years.

TABLE OF CONTENTS

TABLE OF CONTENTS (continued)

LIST OF TABLES

LIST OF ILLUSTRATIONS

LIST OF ILLUSTRATIONS (continued)

NOMENCLATURE

ℓ_s (SL)*	length of supply channel
ℓ_c (CL)	length of control channel
d (D)	depth of supply and control channels
W (W)	width of supply and control channels
h (B)	half width of supply and control channels
V_s (VS)	average supply velocity
V_{CL} (VCL)	average left control velocity
V_{CR} (VCR)	average right control velocity
Q_s (QS)	Supply flow rate
Q_{CL} (QCL)	left control flow rate
Q_{CR} (QCR)	right control flow rate
P_s (PS)	supply pressure
P_L (PL)	supply channel exit pressure
P_{CL} (PCL)	left control pressure
P_{CR} (PCR)	right control pressure
P_4 (P4)	left control channel exit pressure
P_5 (P5)	right control channel exit pressure
V_3 (V3)	resultant radial jet average velocity
ϕ (PHI)	deflection angle of resultant jet (as measured with the verticle)
θ (THETA)	$90 - \phi$
α (ALPHA)	deflection angle of wall jet
ρ (RHO)	density

* Computer program nomenclature

μ (MU)*	viscosity
g	gravitational constant
X	distance from the impact plane along the wall
Y	distance from the wall along the impact plane
Z	distance perpendicular to the plane of XY
in. oil	pressure -- inches of red oil (sp. Gr. 0.834)
in. Hg.	pressure -- inches of mercury (Sp. Gr. 13.596)
Sp. Gr.	specific gravity
psig	gage pressure -- pounds per square inch
PSI	pounds per square inch
CFH	cubic feet per hour
R_e	Reynolds Number

*Computer program nomenclature

SUMMARY

The current investigation explored a new concept in fluidic amplification. This concept was the modulation of a radial wall jet formed by two plane impacting wall jets with transversely and perpendicularlly placed control jets. This was the first known venture using two impacting wall jets to form the power jet of a proportional fluidic amplifier.

An integral control volume analysis was used to analytically predict the resultant jet deflections. The supply pressure and flow were measured. The control pressures used were such that the flows in the channels were laminar. Thus, the pressures and velocities at the exit of each channel, which were the control volume boundaries, were easily calculated.

A test system capable of measuring the input parameters as well as the resultant radial jet profiles was designed and built.

Several test devices were designed and built using a photo etching process. After studying these preliminary designs, a modified device was constructed, tested, and evaluated. The experimental results agreed with the calculated jet deflection angles which were very small. The radial jet velocity profiles were the same as a jet issuing from a slot.

It was concluded from the results of these investigations that placing the control jets parallel and in close proximity to the wall jets would not produce large deflection angles for small control signals which were necessary for a high gain fluidic amplifier.

Using the knowledge gained during this work a new location for the control jet was proposed. The control jet was placed perpendicular to the wall jet at a point out of the impact region of the wall jets. Again, an integral control volume analysis was used to predict the jet deflection angles. The computed angles for the proposed new configuration were found to be one hundred percent larger than those of the previous configuration. It was proposed that this perpendicular configuration would be a suitable configuration for use as an impact proportional fluidic amplifier in future investigations.

CHAPTER I

INTRODUCTION

Background

Fluidics, as a technology, has successfully passed through several critical stages of development in the past decade. It is continuing to overcome more shortcomings at the present time. In the field of proportional or analog fluidic control systems, there has always existed a demand for techniques to increase the pressure gains of fluidic amplifiers. In response to this, control engineers have developed techniques to stage several fluid amplifiers in cascades, thus delivering higher gains. The inherent limitation with this approach has been the problem of impedance matching of amplifier stages. In order for the cascaded stages to perform satisfactorily, only limited pressure and flow combinations at the interconnection station may be used. This, in turn, results in a reduced gain increase than should be expected when two stages are cascaded.

Another problem with multiple staging is the decay of signal to noise ratios. As the pressure gain of two stages in cascade is higher than a single stage, so is the noise to signal ratio. This points to the necessity of devising fluid amplifiers with higher gains, thus relieving some staging requirements.

Currently, the basic technique of jet field modulation is the so-called beam deflection method. In this technique, a power jet is deflected by two transversely impinging low energy control jets,

normal to the power jet, one on each side of it. The resultant pressure changes in the downstream jet receivers correspond to pressure amplification of the control jet pressure differential.

The current work consists of an investigation to study new ways of jet field modulation which would result in new amplifier configurations, yielding higher gains.

Prior investigations with directly impacting axisymmetric power jets modulated by concentric annular control jets had indicated that substantially higher pressure gains could be achieved with this technique than with the conventional jet beam deflection technique (1), (2), (3). From this experience, it was proposed that this technique be modified to two dimensional impacting power jets, rather than axisymmetric ones. To modulate the impact plane formed by the two impacting power jets, two control jets were placed parallel to the power jets and transverse to the impact plane.

The purpose of this research was to evaluate the suitability of the two dimensional impact configuration as a proportional fluidic amplifier.

Wall Jet Theory

There has been considerable effort expended in the study of wall jets both with and without parallel flow.

Wall jets, radial or plane, laminar or turbulent, are formed when a jet of fluid impinges onto a surface at an angle from 0 to 90 degrees. When a axisymmetric jet of air strikes a surface at right angles and spreads out radially over it, it forms what is termed a

radial wall jet. Such a flow is produced by a downwards - directed jet spreading out over the ground. If a plane jet impinges on a fixed plate parallel to the direction of flow, a wall jet is produced on each side of the plate. The jet velocity profiles can be calculated since it is possible to perform the integrations analytically. Similar velocity distributions are applicable for both radial and plane wall jets and for both laminar and turbulent flow (4). Figure 1 shows the fully developed similar wall jet velocity profiles (4), (5). Boundary conditions on the surface wall jet are such that the velocity at the wall and also outside the boundary layer are zero. Thus, the velocity profile must have a maximum. The free and solid boundaries generate considerable interest, since the flow has both a jet-like property and also is influenced by the wall.

The two dimensional tangential wall jet was studied experimentally by Sigalla (6). His data were correlated in a manner analogous to that of a turbulent boundary layer on a flat plate. The boundary layer thickness was found to vary linearly in the direction of flow, making an angle of 3.7 degrees with the plate and passing through the center of the outlet of the jet. Also, it was found that the velocity varied as a power of x with an exponent of minus one-half.

The study of wall jets with parallel flow has been accomplished by dividing the flow region of interest into a number of subzones and matching the conditions at the boundaries of the subzones. The incompressible, turbulent, two-dimensional plane wall jet was characterized as having three major flow regions as shown in Figure 2 (7). First, a constant velocity core is maintained near the exit. Second, an outer

Note: η is a function of x and y.

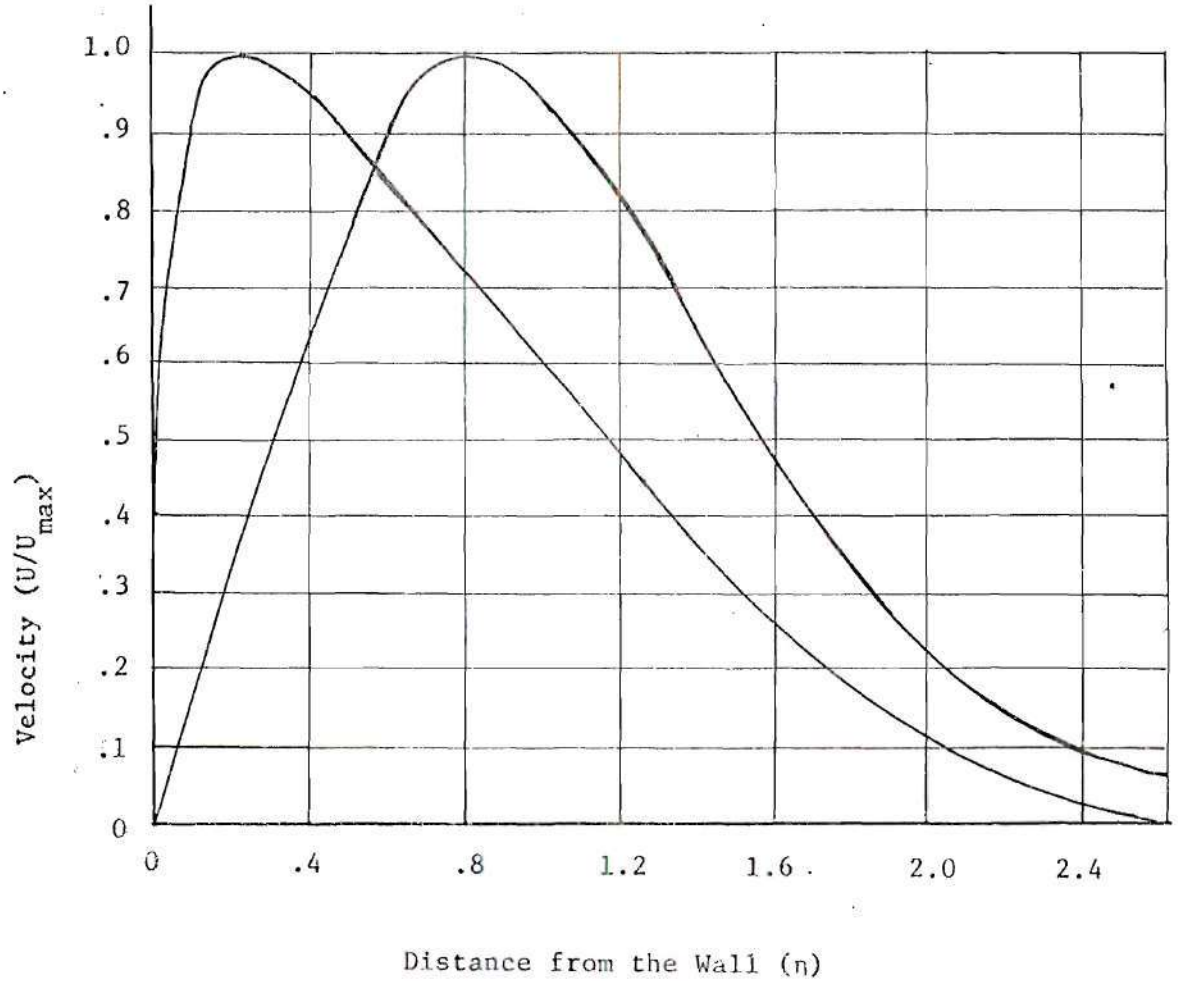

Figure 1. Wall Jet Velocity Profile

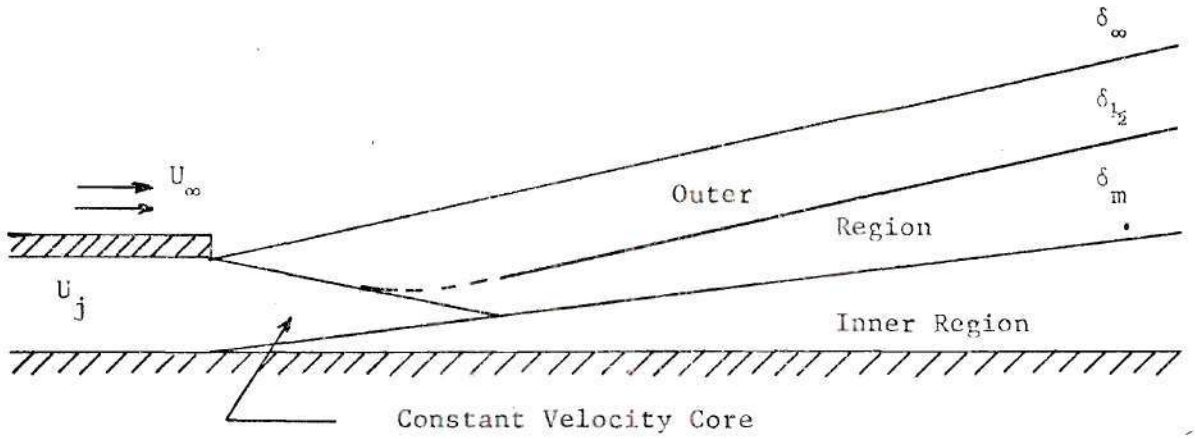

Figure 2. Incompressible, Turbulent
Two-Dimensional Plane Wall Jet

region that behaves as a free jet, decaying from the maximum velocity out to the parallel stream velocity through the action of mixing with the parallel stream. This outer layer appears to possess many of the characteristics of the free-mixing flow of a plane, turbulent free jet discharing into a moving stream. Third, an inner region that behaves as a boundary layer, decaying from a maximum velocity at δ_m into zero velocity at the wall. The maximum velocity is common to both the inner and outer region and defines the boundary between them, δ_m.

Further details of the wall jet theory can be found in the literature (8), (9), and others.

Impact Phenomena

Previous investigations concerned with axially opposed impacting jets have been on axisymmetric jet modulation. This impact phenomena was used as a new concept in fluid amplification. It was called the impact modulator and was first reported by Bjornsen (10).

If two axially symmetric jets were placed in opposition to each other along their center lines, flow from the jets would impact radially, forming an impact plane between the two jets as shown in Figure 3. The location of this impact region would depend on the momentum flux difference between the jets issuing from the nozzles and the pressure gradients in the impact region. By increasing the momentum of one of the jets, the radial impact region would move away from this jet toward the opposing jet. If a circular collector was placed concentric with the centerline in the region between the jets, the impact momentum could be recovered. Thus, by changing the power level of one of the

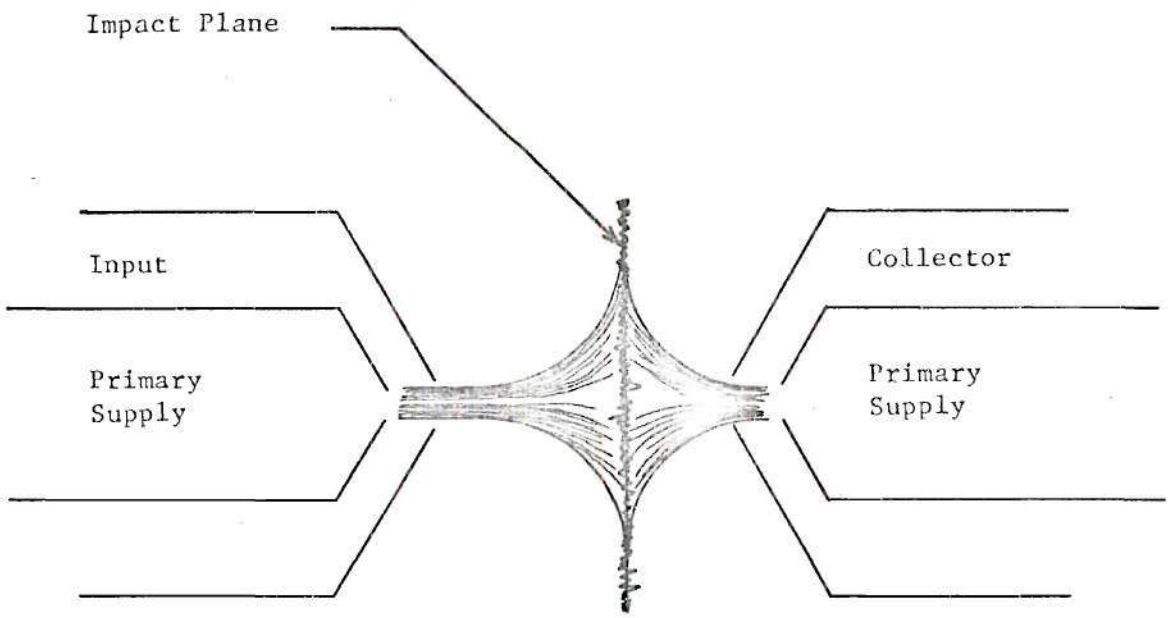

Figure 3. Radial Impact Plane of Direct Impact Modulator

jets,, the impact region would move relative to the collector and a modulated output would be obtained.

Further, this modulation could be achieved by an input imposed through an annulus surrounding one of the jets, this input would focus the supply jet, moving the impact region, and the ouput could be collected around the opposing jet through a similar annulus. This direct impact modulator was shown to possess good pressure and flow gains (2).

The success with axisymmetric impacting jets as the power supply for use as a fluidic amplifier has lead to the question of whether or not impacting two dimensional jets could be used with the same success.

Impacting Wall Jets

A two dimensional configuration fluidic amplifier which corresponds to the axisymmetric impact modulator was developed as shown in Figure 4. In this impacting wall jet fluidic amplifier two supply power wall jets were formed from the same stagnation region, and thus the wall jets had equal momentum. This made the impact plane coincident with the centerline of the device which had symmetrically designed right and left sides about the centerline. The resultant radial jet was formed with the impact plane as its centerline. This radial jet was to be modulated by two control jets which were parallel to the wall jets and transverse to the impact plane. Two output receivers were placed one on each side of the impact plane or the centerline of the device and downstream from the region of radial jet formation.

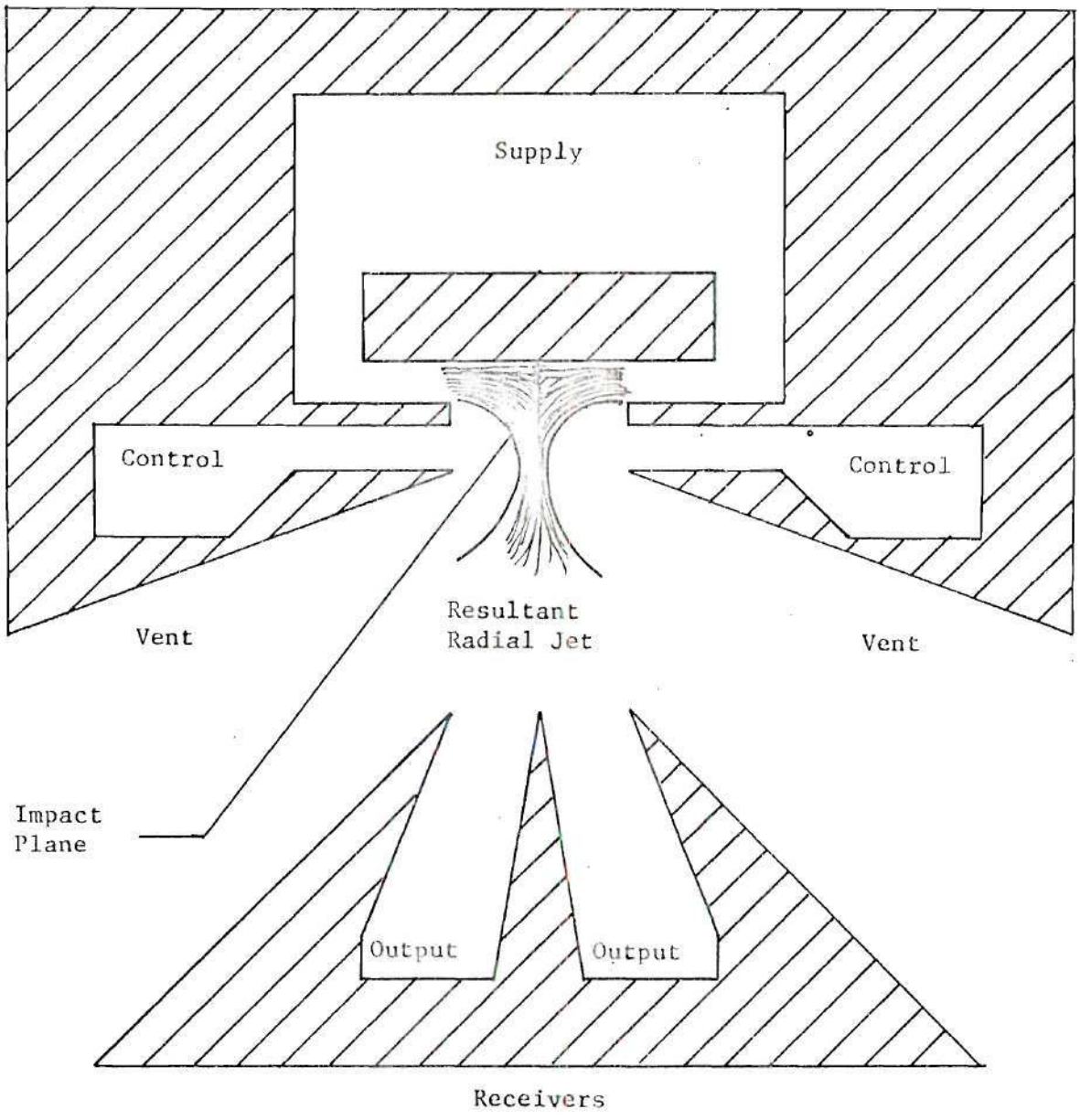

Figure 4. Impacting Wall Jet Fluidic Amplifier Configuration

The significant variables of operation of this type device were supply pressure and flow, control pressure and flow, sizing of supply and control channels, seperation distance of the outlet of these channels, vent size and configuration, output pressure and flow, sizing of the output receivers, and the location of these output receivers.

There was no prior investigations of this configuration amplifier or any similar configuration, nor was there any previous work with impacting wall jets with or without parallel flow.

CHAPTER II

THE TEST DEVICE AND TEST SYSTEM

Device Design

It was felt that several geometrical configurations would have to be tested in order to understand the geometrical parameter influences. Thus, several configurations were fabricated and subjected to preliminary tests. These were of two different types; first, an impacting wall jet fluidic amplifier, and second, impacting wall jets with parallel control flow for velocity field measurements.

Representative of the first type was Configuration Number 8 as shown in Figure 4, schematically, and in Figure 17 of Appendix E for details. Supply and control regions were made very large relative to the channel size to eliminate the region entrance effects and to provide low entrance velocities into the channels. The entrances to the supply and control channels were designed for minimum losses and to promote fully developed channel flow in a relatively short distance. All channels were made five channel widths long to give similar pressure - flow characteristics. This channel length was sufficient to yield fully developed laminar channel flow. The depth of the channels and entire flow region including vents and output receivers was the same, 0.040 inch. The width of both the channels was 0.026 inch which gave an aspect ratio of 1.538. The total distance between both the supply channel exits and the control channel exits was ten channel

widths; again this was to allow the wall jet development.

The vents were made large to eliminate the resultant radial jet attachment to the vent walls. An angle of 25 degrees was used in configuration Number 8 which was sufficient to prevent wall attachment. The output receivers were placed slightly greater than twenty-five channel widths downstream in Configuration Number 8. This configuration represented the best obtained from numberous test amplifiers. Vent and receiver design were dependent on each other such that a larger vent required the receivers to be placed further downstream.

The second type device as shown in Figure 5, actual size, and in Figure 17 of Appendix E for details was for investigating the resultant radial jet formed by two impacting axially opposed wall jets with parallel control flow. The geometry for this device was essentially the same as the previous device, the difference being the angle of the vent wall. This angle was decreased from the 25 degrees of the first configuration to 10 degrees in this second configuration. This caused the control stagnation region to be changed, and the control channel length to be increased. The increased length had only a slight effect on the operating characteristics, the change being a small increase in the pressure drop in the control channel.

Device Fabrication

Fabricating fluid amplifiers by machining the flow passages has proved unsatisfactory. At best, it is very time consuming, uneconomical, and marginally accurate. Since many test components had to be fabricated, a new way of fabrication had to be devised. The technique

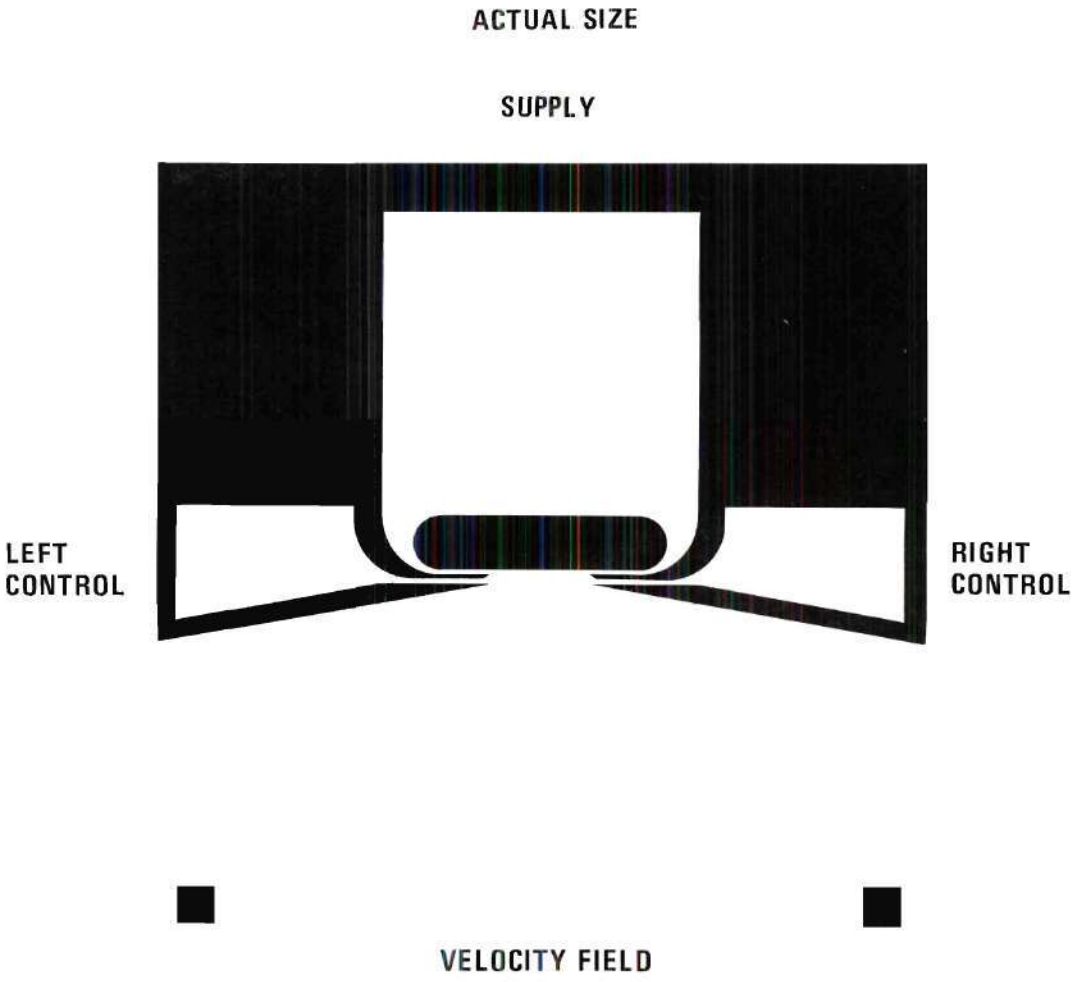

Figure 5. The Impact Configuration Test Device.

of photo etching was used.

In this method, first an oversized cutout of the configuration was made of a special plastic sheet, Para-Paque, Zip-A-Tone. A negative of this cutout was made with a Graflex graphic art camera, any reduction in the size of this coutout could be achieved on the photographic plate by varying the size of the cutout and/or the size of the image on the negative. For the devices tested a 20" x 20" cutout was made, and a 4" x 4" image was made on the negative. This gave a reduction in size by a factor of five which made a high quality negative with precise dimensions and straight channels. The film used to make the negative was Kodalith Ortho Film, Type 3, and extremely high-contrast, orthochromatic film which gave high-quality line negatives with exceptionally wide exposure and development latitude and excellent size holding. This film was then developed and a positive was made on Dupont-Cronar Ortho D film, a high contrast film which has a density of at least 4.0 in the opaque areas of the positive.

The positive was placed in contact with an unexposed Dycril plate that had not been preconditioned in a carbon dioxide atmosphere. Dycril had a thin layer of photosensitive plastic (photopolymer) bonded to a flexible steel backing. Type 60 Dycril was used which has a 0.061 inch total thickness and 0.040 inch relief depth. The positive and the Dycril plate were then drawn into intimate contact in a flat vacuum frame. The plate was exposed, through the negative, to ultraviolent light as shown in Figure 6. Where this light strikes the Dycril plate, it made the photopolymer insoluble. Unexposed, soluble areas were then washed away by a spray of dilute sodium hydroxide and water. No acid

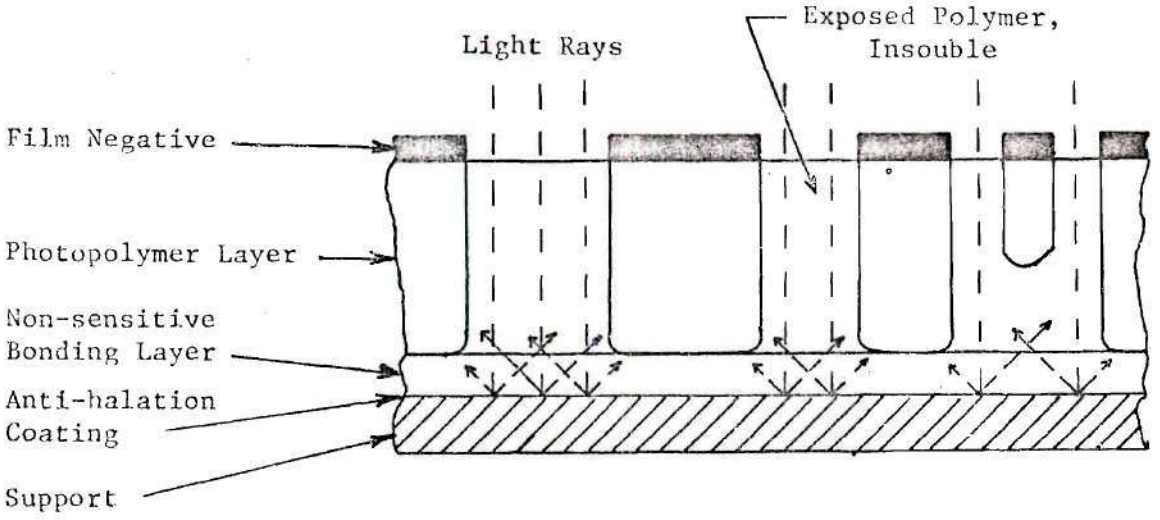

Figure 6. Exposure of Dycril

etching was required. After drying, the plate was completely fabricated. The time required was approximately twenty minutes from exposure through drying.

To this etched plate a bottom plate of acrylic plastic was added for support. A top cover plate of plexiglass with input and output fittings for connecting plastic tubing for air flow was screwed to the Dycril plate. The device in this form became ready for testing.

Test System

As there were two different types of fluidic devices, slight modifications were necessary to adapt the test system to both test units.

The test system was designed for testing the type fluidic amplifier of Configuration Number 8. This system provided instrumentation and pressure and flow control for supply, right and left outputs as shown in the schematic, Figure 19 of Appendix E.

A modified test system which was able to test the type fluidic device for velocity field measurements provided instrumentation and pressure and flow control for supply and right and left control only, plus a movable pitot tube for velocity surveys as shown in Figure 7 and in the schematic, Figure 20 of Appendix E.

Filtered and regulated compressed air was supplied through a large stagnation tank, volume 2.77 cubic feet, to the test system. Shutoff valves and flow control valves were provided with a bleed valve vented to the atmosphere to provide finer flow adjustments. The pressure taps to all inputs and outputs were symmetrically places as close as

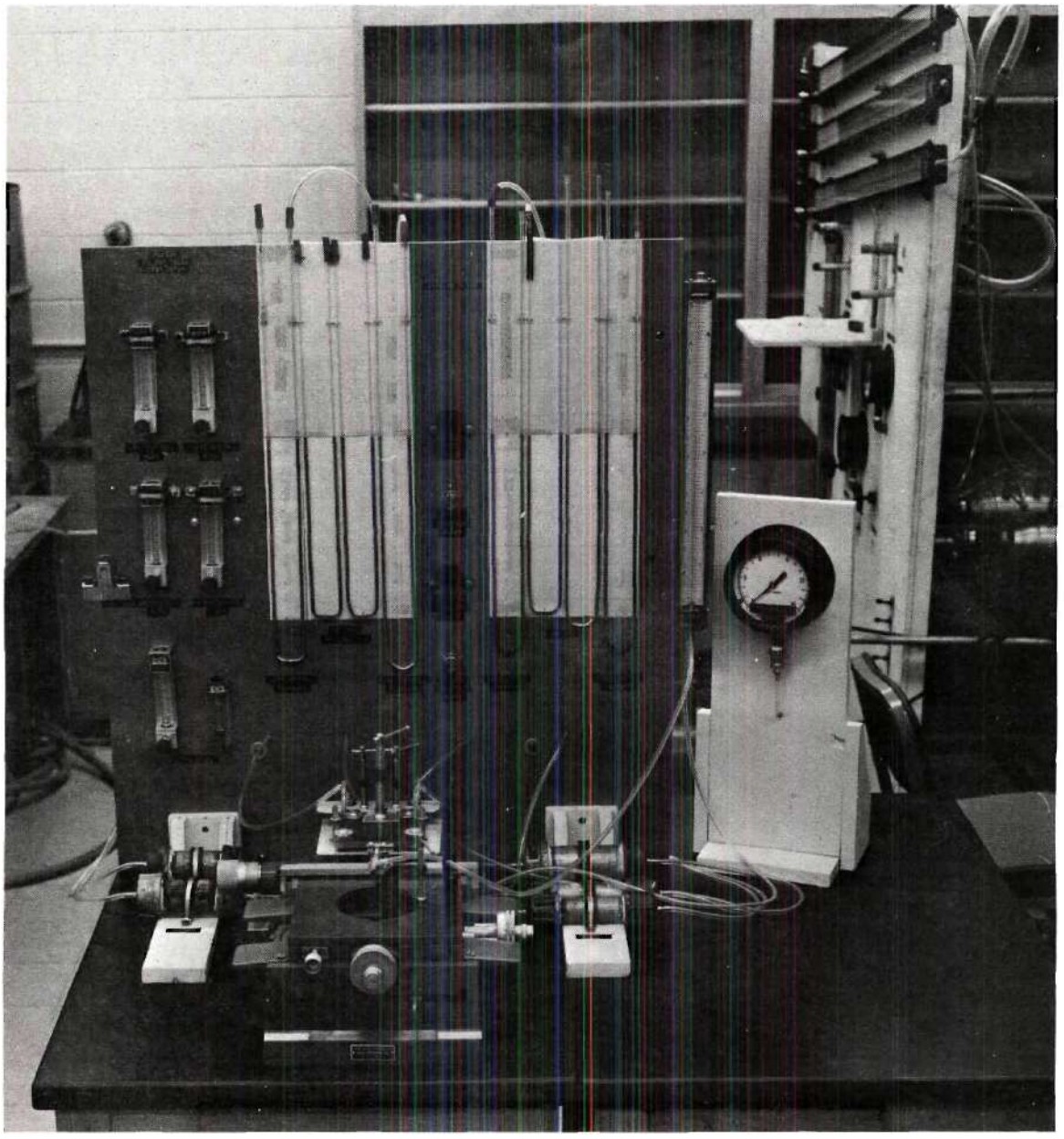

Figure 7. Complete Test Setup.

practicable to the fluidic device.

The test instrumentation for flow rate and pressure measurements was as shown in Figure 8. The range of pressure provided by the pressure instrumentation, which were U-tube manometers, was twenty inches of both red oil, specific gravity 0.834 and mercury, specific gravity 13.6. This corresponded to a range of 0 to .6 psi and 0 to 9.84 psi respectively. These ranges were found to be adequate for all studies conducted. The supply pressure was monitored only with a mercury manometer since the supply pressures were always an order of magnitude greater than the control and output pressures. The flow rates were obtained using E/C Purge Meters of the Brooks Instrument Division in units of cubic feet per hour (CFH) with ranges as follows: supply flow, 0-90 CFH; control flow, 0-10 CFH; output flow, 0-10 CFH. Right and left control and output flows were presented with equal impedance since both right and left line lengths were made exactly equal.

For the velocity profile investigations a pitot tube was made from a two inch long, twenty-five gage hypodermic needle by squaring and deburring the end. This configuration was not a standard shape for a pitot or total pressure probe which would give an exact measurement of the velocity, but it did give a good measurement for relative velocities from point to point in the flow field. This pitot tube was mounted on a two dimensional micrometer drive table which traversed the pitot tube in the x and y directions with an accuracy of one ten thousandth of an inch. The pitot tube was connected to a plastic

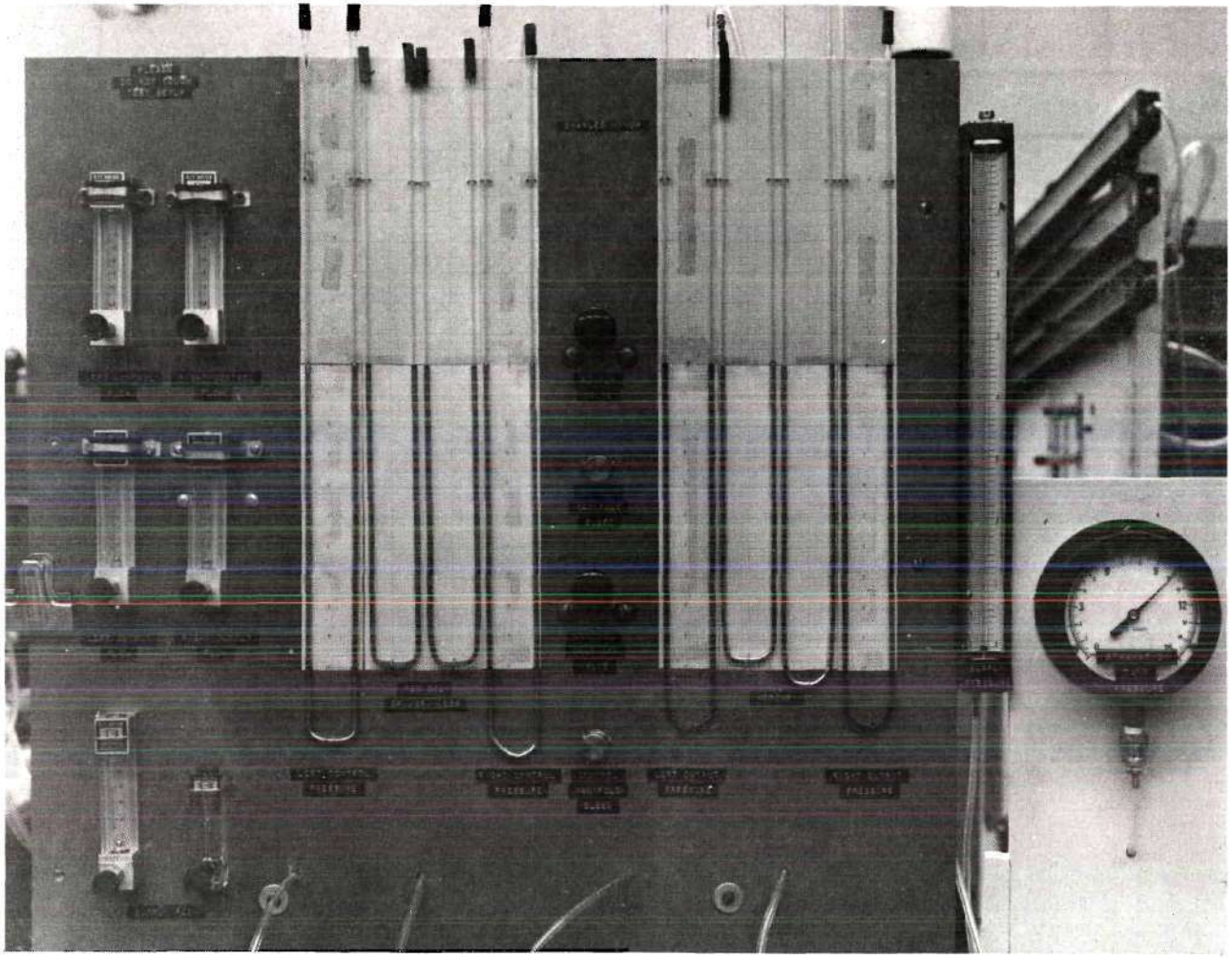

Figure 8. Test Instrumentation.

tube which was mated to one side of an U-tube manometer as shown in Figure 9.

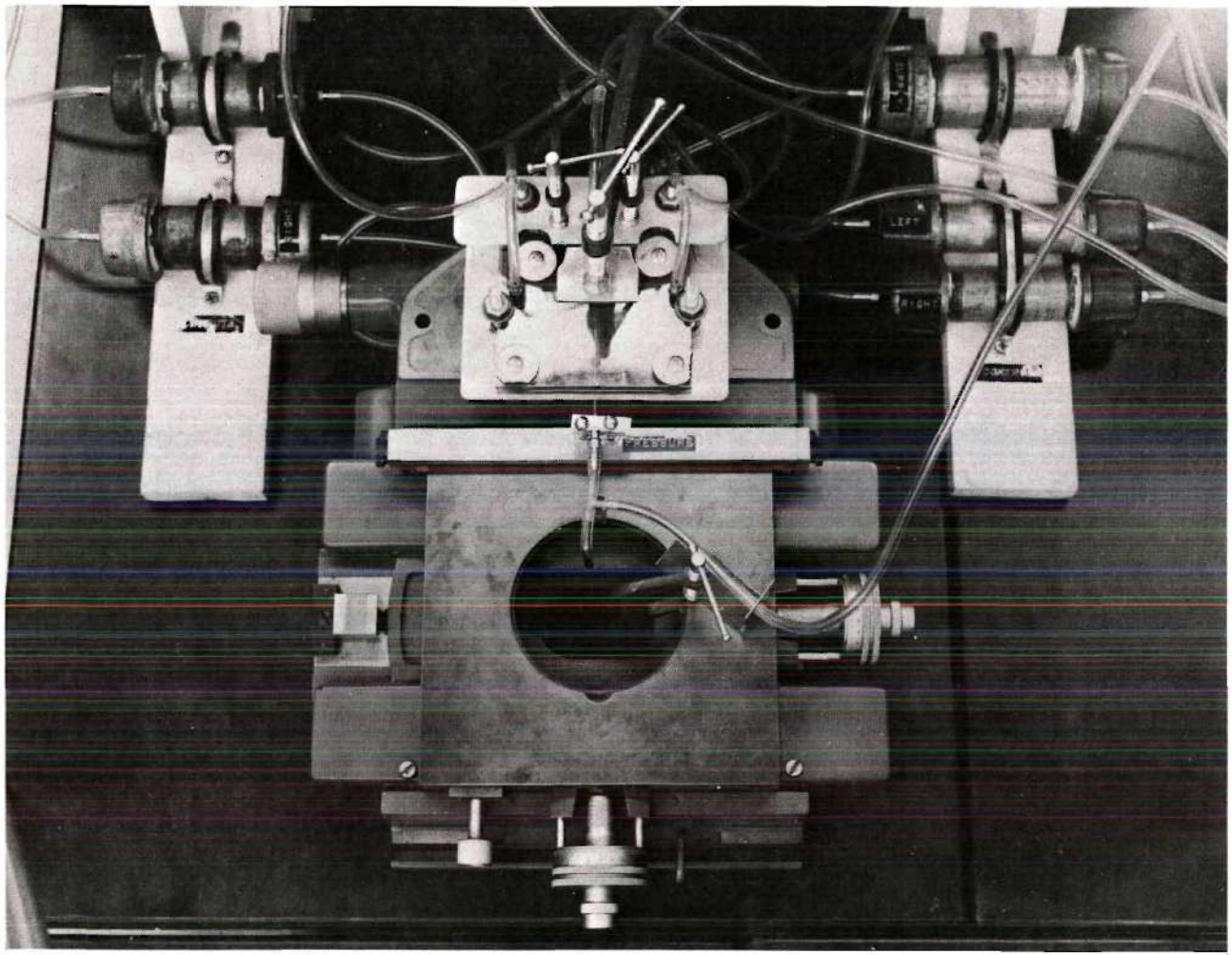

Figure 9. Test Drive and Pitot Tube.

CHAPTER III

EXPERIMENTAL PROCEDURE

Initial Investigations

The following systematic procedure was used for static testing of the fluidic amplifier Configuration Number 8 and all similar amplifier configurations.

1. A supply pressure was selected.
2. Pressures at the control ports were adjusted to a percent of the supply pressure. This was the bias level.
3. The load valve was kept wide open at minimum output impedance.
4. Right control pressure (PCR) plus left control pressure (PCL) was kept constant at the bias level.
5. Then, PCR was increased and PCL was decreased by the same amount so that a ΔP was obtained between the control channels and still the control bias level was maintained at the same average percent of the supply pressure as was established in step 2.
6. This was continued for various ΔP's.
7. The output pressure and flows were recorded, and this gave the static characteristics for the minimum load condition.
8. Different bias level were selected and steps 2. through 7. were repeated.

Numerous amplifier configurations were subjected to preliminary tests using this systematic test procedure, and their static gain characteristics were determined. It was found that the attachment characteristics of the impact stream required significant changes in the vent and receiver geometry for stable nondigital operation with reasonable pressure recovery. Configuration Number 8 evolved as a

design without jet attachment to the vent walls and, therefore, had stable nondigital operating characteristics.

A supply pressure of 1 psi was selected since this pressure provided an average velocity in the control channel of 192 ft./sec. or a Mach Number of 0.172. The velocity was determined by using the relation $V = Q/A$. This velocity was well within the range of air velocities which could be considered as incompressible flow. Also, the supply pressure of 1 psi caused and extremely small pressure drop of approximately 0.02 psi or 1.0 inch of oil as shown in the calculations of Appendix A. A velocity of 192 ft./sec. for the supply channel gave a Reynolds Number of 2600.0 based on the channel width which was in the intermediate range between laminar and turbulent flow. Laminar flow was assumed only for pressure drop calculations.

The experimental investigation of the fluidic amplifier Configuration Number 8, revealed that it was not operating satisfactorily. Pressure gain was determined as the ratio of the change in output differential pressure for a given change in control differential pressure. Various supply pressures were attempted. As representative of these tests the results from using a supply pressure of 2 in. Hg. were recorded. Control bias levels of 5%, 10%, 12.5%, and 23% were used. For pressure amplification, pressure gains should be greater than one, that is the change in output should be larger than the change in the input. As shown in Tables 8, 9, 10, and 11 of Appendix F and Table 1, the Configuration Number 8 did not operate as an Amplifier at any control bias level.

Since the results of these tests were significantly below the

Table 1. Configuration Number 8 Amplifier Characteristics

Bias Level	Data Point Number	Change in ΔP Control	Change in ΔP Output	Change in ΔQ Output	Pressure Gain
5.0%	1-2	1.0	0.1	0.1	0.1
	2-3	1.0	0.3	0.6	0.3
	3-4	1.0	0.4	0.5	0.4
	5-6	1.0	0.1	0.1	0.1
	6-7	1.0	0.5	0.2	0.5
10.0%	1-2	1.0	0.3	0.0	0.3
	2-3	1.0	0.2	0.7	0.2
	3-4	1.0	0.4	0.3	0.4
	4-5	1.0	0.4	0.8	0.4
	5-6	1.0	0.3	0.2	0.3
	6-7	1.0	0.6	0.3	0.6
	8-9	1.0	0.2	0.1	0.2
	9-10	1.0	0.1	0.3	0.1
	10-11	1.0	0.2	0.1	0.2
	11-12	1.0	0.0	0.0	0.0
12.5%	1-2	1.8	0.5	0.7	0.28
	2-3	2.0	0.7	1.0	0.35
	3-4	2.0	0.65	0.5	0.33
	4-5	2.0	0.45	0.5	0.23
	5-6	1.0	0.3	0.3	0.30
	7-8	2.2	1.0	-0.8	0.45
	8-9	1.6	1.3	-0.1	0.81
23.0%	1-2	2.0	0.7	0.7	0.35
	2-3	2.0	0.7	0.8	0.35
	3-4	2.0	0.6	0.7	0.30
	4-5	2.0	0.9	-0.1	0.45

expected pressure gains, it was necessary to instigate an investigation to precisely determine the effects of control flow and pressure on the impacting wall jets. This was obtained from velocity field surveys. Knowing the velocity profiles in the entire region of the impacting wall jets and the resultant radial jet would form the basis for a precise design of the vent and jet receivers.

The Test Spectrum

The resultant radial jet formed by the two impacting wall jets was investigated by traversing the flow field with a pitot tube. The pressures measured were proportional to the total pressure of the jet and since the static pressure was constant in a radial jet the measured pressures were proportional to the radial jet velocity.

A supply pressure of 1 psi was selected to correspond to that used in testing Configuration Number 8. A control bias level of 10% was selected since the tests of the amplifier indicated slightly larger gains for this control bias level than any of the other bias levels.

The velocity profiles exhibited the characteristics of a radial jet. The geometrical centerline velocity decreased with increasing distance downstream from the impact region. The jet, also, demonstrated jet spreading due to viscous effects as shown in Figure 10 which was derived from the data of Table 12 of Appendix F. Entrainment was particularly evident from the negative pressures outside the radial jet edge as shown in Table 12 in Appendix F. Figure 10 was selected as representative of the radial jet characteristics; the radial jet velocity profiles with other control jet pressures had the same characteristics with the jet

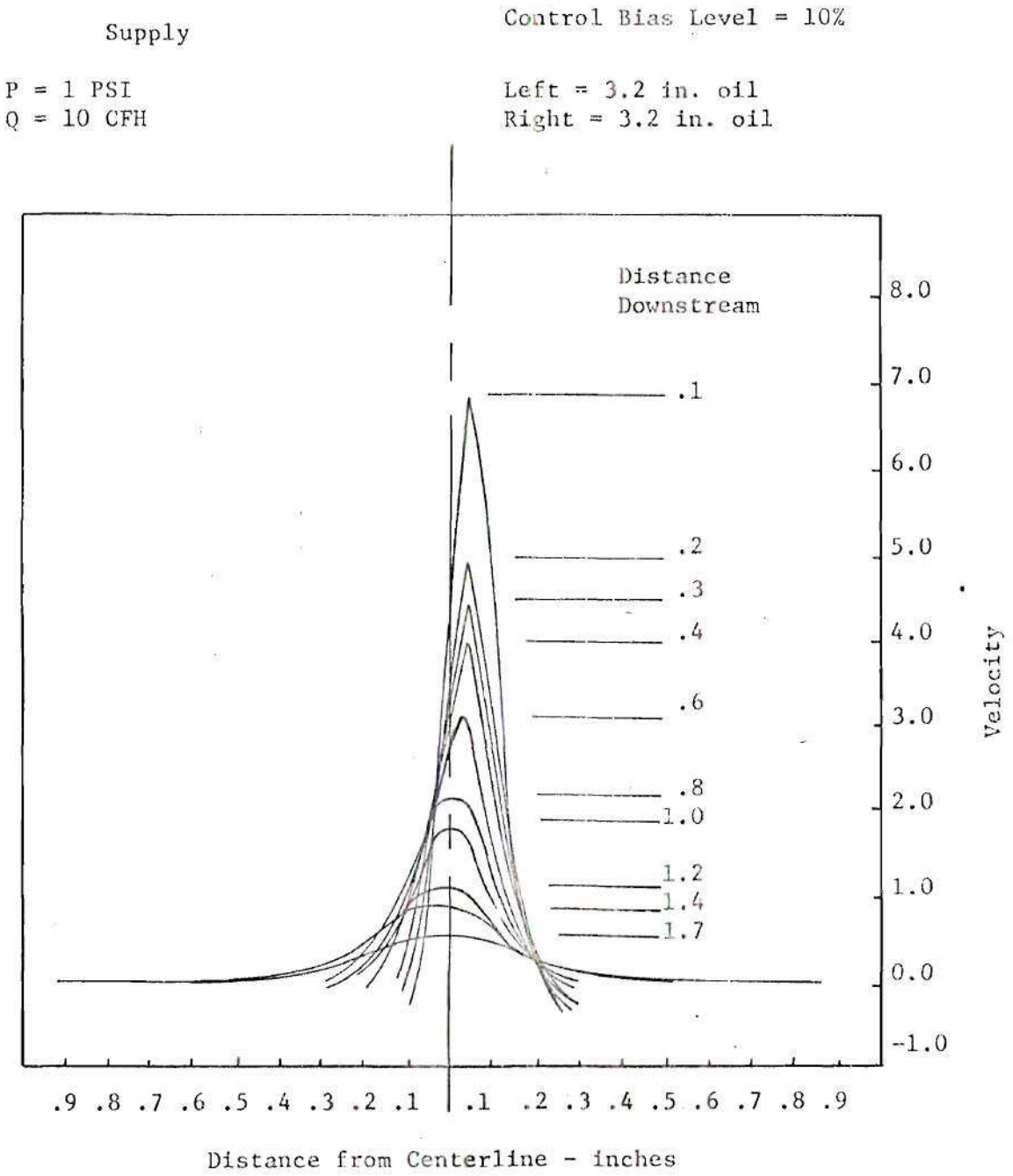

Figure 10. Resultant Radial Jet Velocity Profiles

centerline deflected away from the control jet with increased pressure as shown in Tables 12, 13, 14, 15, and 16 of Appendix F. These jet profiles were to be important in designing the output receivers for maximum pressure recovery including the size and location of the center splitter and the output ports.

The significant parameter in predicting the pressure gain of a fluidic amplifier using this configuration for both supply and control flows was the deflection angle as a function of control differential pressure. Table 2 was obtained from the data of Tables 12, 13, 14, 15, and 16 of Appendix F. The deflection angle was 2.78 degrees for equal control jet pressures of 10% bias level on each, and the angle increased to 7.34 degrees for control jet pressures of 3% bias level on the left control channel and 17% bias level on the right control channel for a total deflection angle of 4.56 degrees. Experimentally the deflection angle increased in the range 0.65 degrees to 1.50 degrees for each discrete change in the control differential pressure; this corresponds to a 0.02 degree to 0.20 degree per inch of oil (specific gravity 0.834) control differential pressure increase.

Control Channel Characteristics

The control flow rates for the 10% control bias level selected were below the range of the flow meters. Therefore, an investigation was undertaken to determine the control channel flow rate vs. inlet pressure characteristics.

The following systematic procedure was used for testing the control channels.

Table 2. Jet Deflection Data

Control Pressure PCL in. oil	PCR in. oil	Jet Centerline @ .1" downstream	@ .9" downstream	ϕ degrees
3.2	3.2	+.038	-.008	2.78
2.9	3.5	+.038	-.018	4.00
2.3	4.1	+.038	-.035	5.21
1.7	4.7	+.035	-.059	6.70
1.1	5.3	+.033	-.070	7.34

Note: 1. + is right; - is left.

2. ϕ is the angle between the radial jet centerline and the verticle.

1. Set supply pressure at zero. Close supply shut-off valve.

2. Set both left and right control flow at zero.

3. Increase right control flow by one increment and record right control pressure.

4. Repeat step 3 several times.

5. Repeat steps 2, 3, and 4 with right control set at zero and increasing left control flow.

6. Repeat steps 2, 3, and 4 except increase both left and right control flows by the same increment keeping the flow rates equal.

The results of these tests were recorded in Table 17 of Appendix F and in graphical form in Figure 11. From these data the control characterists in the very low pressure-flow region were determined.

Referring to Figure 11 for a flow rate less than 1.0 CFH, the flow-pressure characteristics were assumed linear. That is:

$$P = \text{Constant } Q \tag{1}$$

Again referring to the figure, it was seen that:

$$PCL = .3\ QCL \tag{2}$$

and

$$PCR = .2\ QCR \tag{3}$$

or in units of inches of oil and CFH as the previous equations:

$$PCL = 4.89\ QCL \tag{4}$$

and

$$PCR = 3.26\ QCR\ . \tag{5}$$

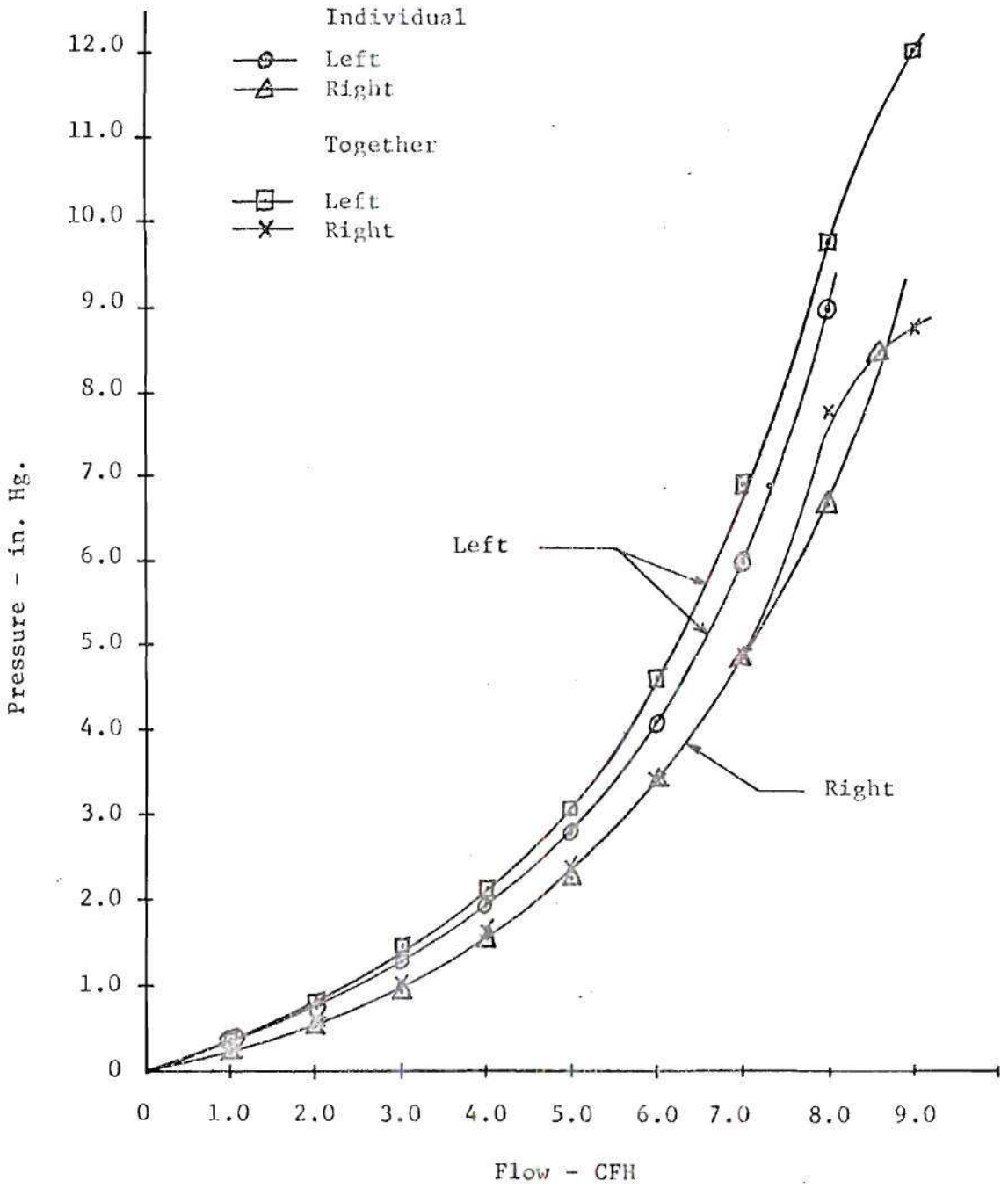

Figure 11. Control Channel Pressure vs. Flow Characteristics

These equations were used for left and right control characteristics respectively for all investigations in which the control flow rate was less than 1.0 CFH.

CHAPTER IV

ANALYTICAL INVESTIGATIONS

Control Volume Analysis

A detailed analysis of impacting turbulent wall jets which were used in this investigation would necessitate extensive empirical information due to the complex and untractable mathematics involved. However, an analysis which would consider the overall phenomena would not necessitate extensive empirical data. For this reason an integral control volume analysis was applied to two different impacting wall jet fluidic amplifier configurations.

A control volume was defined as an arbitrary volume, in space, through which fluid flows. Thus, the fluid occupying the control volume changed from instant to instant. The boundary of the control volume was a bounded surface. For the present problem a finite control volume was employed.

To make use of the control volume concept for this analysis, it was necessary to write the law of conservation of mass, Newton's second law of motion, and the first law of thermodynamics in a form applicable to a control volume (11).

Assuming a continuous medium the equation of continuity for a control volume is:

$$\int_{\substack{\text{control}\\\text{volume}}} \frac{\partial \rho}{dt}\, d\text{vol.} = - \int_{\substack{\text{control}\\\text{volume}}} \rho \vec{V} \cdot d\vec{A} \qquad (6)$$

The momentum theorem, or Newton's second law, for a control volume is:

$$\Sigma\vec{F}_{drag} + \Sigma\vec{F}_{body} + \int_{\substack{control\\surface}} \vec{P}\vec{N}dA =$$

$$\frac{\partial}{dt} \int_{\substack{control\\volume}} \rho\vec{V}\ dvol. + \int_{\substack{control\\surface}} \rho(\vec{V} \cdot d\vec{A})\ \vec{V} \qquad (7)$$

The first law or energy equation, for a control volume is:

$$\frac{dq}{dt} - \frac{dWs}{dt} = \int_{\substack{control\\surface}} (e + pv)\ \rho\vec{V} \cdot d\vec{A} +$$

$$\frac{\partial}{dt} \int_{\substack{control\\volume}} e\rho\ dvol. \qquad (8)$$

where

$$e = u + \frac{V^2}{2} + gZ \qquad (9)$$

Applying the preceding equations to a simple case of impacting wall jets as with control volume ABCDEFA as shown in Figure 12 resulted in a relatively simple equation for ϕ.

It was assumed that the flow was incompressible and steady with $V_2 \geq V_1$, $P_2 \geq P_1$, $A_1 = A_2 = A$. The pressure of the resultant radial jet at A_3 was assumed as atmospheric. In the immediate vicinity of the Impact region, that is, in the control volume, the flow field was essentially governed by pure momentum and pressure forces and mixing

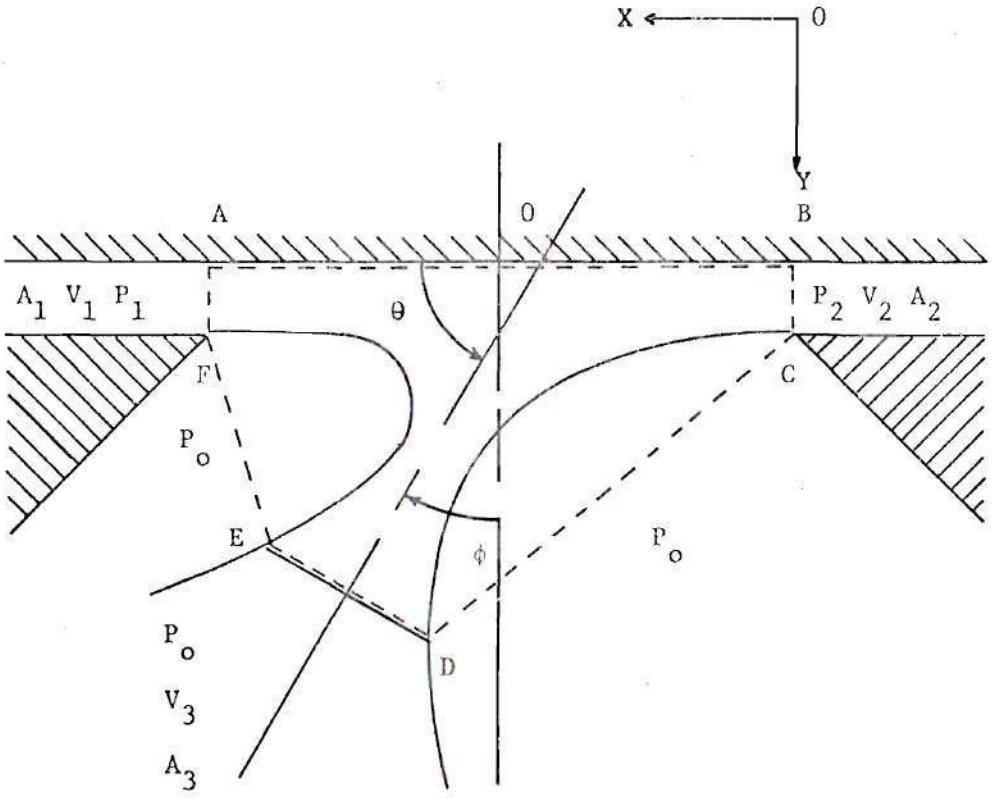

— — — Control Volume Boundary

Figure 12. Impacting Wall Jets

of the jets was not significant.

Summing the momentum in the X - direction:

$$(P_o A_{ED})_X - (P_o A_{DC})_X + (P_1 A_1)_X - (P_2 A_2)_X =$$

$$- \rho (V_1^2 A_1)_X + \rho_2 (V_2^2 A_2)_X - oA_{ED} + oA_{DC}$$

$$- \rho A_3 V_3^2 \cos \theta \qquad (10)$$

simplifying with $(P_o A_{ED})_X = (P_o A_{DC})_X$:

$$A(P_1 - P_2) = A\rho (V_2^2 - V_1^2) - \rho A_3 V_3^2 \cos \theta. \qquad (11)$$

Applying the continuity equation:

$$\rho A_1 V_1 + \rho A_2 V_2 = \rho A_3 V_3 \qquad (12)$$

or

$$A_3 V_3 = A (V_1 + V_2) . \qquad (13)$$

Now, applying the energy equation:

$$\rho A_1 V_1 \frac{V_1^2}{2} + \rho A_2 V_2 \frac{V_2^2}{2} = \rho A_3 V_3 \frac{V_3^2}{2} \qquad (14)$$

simplifying,

$$A (V_1^3 + V_2^3) = A_3 V_3 V_3^2 . \qquad (15)$$

Substituting for $A_3\ V_3$ from the continuity equation:

$$A\ (V_1^3 + V_2^3\ ) = A\ (V_1 + V_2)\ V_3^2 \tag{16}$$

and rearranging,

$$V_3 = \left[\frac{V_1^3 + V_2^3}{V_1 + V_2}\right]^{1/2} . \tag{17}$$

Now, rearranging the continuity equation:

$$A_3 = \frac{A\ (V_1 + V_2)}{V_3} \tag{18}$$

and substituting for V_3 from the preceding equation:

$$A_3 = A\left[\frac{(V_1 + V_2)^3}{V_1^3 + V_2^3}\right]^{1/2} . \tag{19}$$

Next, substituting for A_3 and V_3 in the momentum equation:

$$A(P_1 - P_2) = A\rho\ (V_2^2 - V_1^2\ ) - \rho A\left[\frac{(V_1 + V_2)^3}{V_1^3 + V_2^3}\right]^{1/2}\left[\frac{V_1^3 + V_2^3}{V_1 + V_2}\right] \cos\ \theta \cdot \tag{20}$$

Solving this equation for COS θ

$$\cos\ \theta = \frac{\rho(V_2^2 - V_1^2) + P_2 - P_1}{\rho\left[(V_1 + V_2)(V_1^3 + V_2^3)\right]\ 1/2} . \tag{21}$$

Finally, the complete expression for the deflection angle is:

$$\phi = 90° - \cos^{-1}\left[\frac{\rho(V_2^2 - V_1^2) + P_2 - P_1}{\rho\left[(V_1 + V_2)(V_1^3 + V_2^3)\right] 1/2}\right] . \qquad (22)$$

If the pressues and velocities of the wall jets were known the resultant radial jet velocity and direction were completely determined. These pressures and velocities were at the exit of the channels; therefore the exit conditions had to be determined when the entrance conditions were known. The channels under study were precisely designed and fabricated; thus all necessary dimensions were known.

For laminar flow in a slit the average velocity and the pressure loss in the slit could be calculated by applying the momentum equation if the entrance pressure and the flow rate were known (12).

$$V_{average} = \frac{(P_{entrance} - P_{exit})\, b^2}{3\,\mu\ell} \qquad (23)$$

and,

$$P_{exit} = P_{entrance} - \frac{3Q\,\mu\ell}{2\,d\,b^3} \qquad (24)$$

Where Q, flow rate, and $P_{entrance}$, entrance pressure, were the known parameters.

The validity of the laminar flow assumption was checked after $V_{average}$ was determined by.

$$Re = \frac{\rho V_{average}\, W}{\mu} . \qquad (25)$$

The Reynolds Number, Re, should not exceed approximately 2000; but if large stagnation regions and streamlined entrances were provided, the Reynolds Number could have been slightly larger and still had the flow remain laminar.

Configuration Analysis

The previously discussed control volume analysis was applied to the impacting wall jets with parallel control channels which were transverse to the resultant radial jet with control volume ABCDEFA as shown in Figure 13. This was precisely the configuration which was experimentally investigated. It was known that $A_1 = A_2 = A_4 = A_5 = A$.

Summing the momentum in the X-direction:

$$(P_o A_{ED})_X - (P_o A_{DC})_X + (P_1 A)_X - (P_2 A)_X + (P_4 A)_X$$

$$-(P_5 A)_5 = -\rho(V_1^2 A_1)_X + \rho(V_2^2 A_2)_X - \rho(V_4^2 A_4)_X + \rho(V_5^2 A_5)_X$$

$$- 0\, A_{DC} + 0\, A_{ED} - \rho A_3 V_3^2 \cos\theta \qquad (26)$$

simplifying with $(P_o A_{ED})_X = (P_o A_{DC})_X$:

$$A(P_1 - P_2 + P_4 - P_5 = \rho A\,(-V_1^2 + V_2^2 - V_4^2 + V_5^2)$$

$$-\rho A_3 V_3^2 \cos\theta \qquad (27)$$

Applying the continuity equation resulted in:

$$A(V_1 + V_2 + V_4 + V_5) = A_3 V_3 . \qquad (28)$$

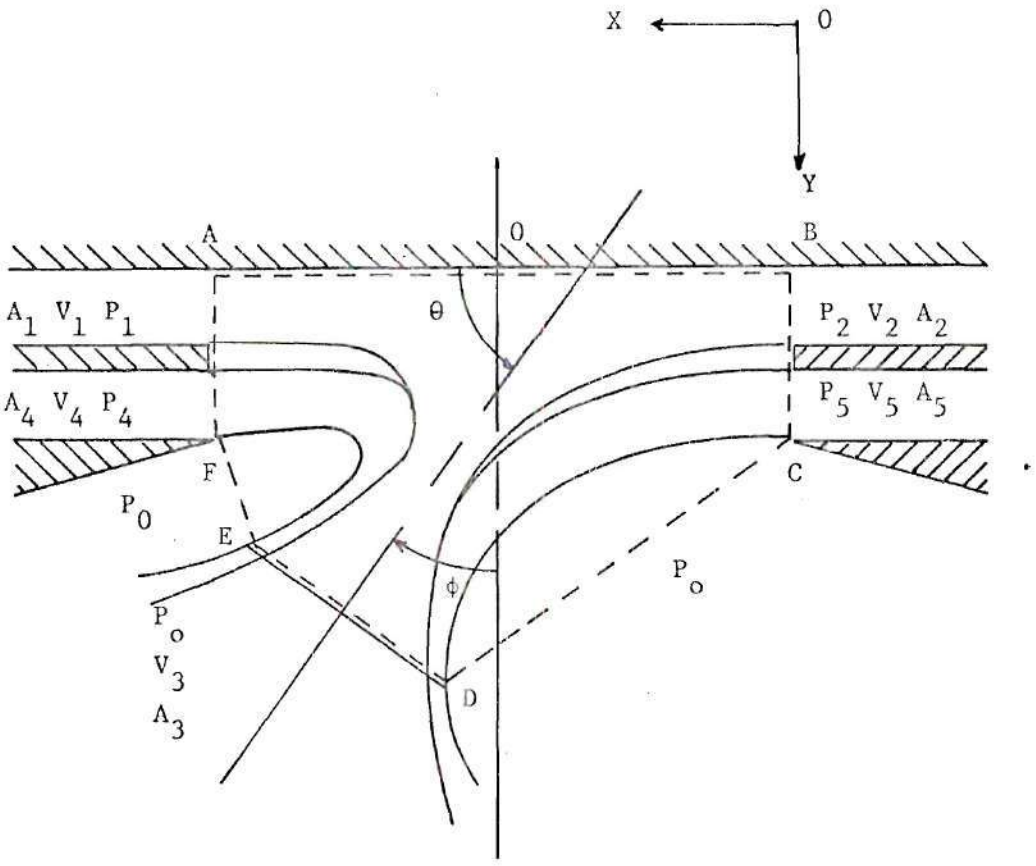

— — — Control Volume Boundary

Figure 13. Impacting Wall Jets with Parallel Control Flow

Now, applying the energy equation and simplifying:

$$A(V_1^3 + V_2^3 + V_4^3 + V_5^3) = A_3 V_3 V_3^2 . \tag{29}$$

Substituting for $A_3 V_3$ from the continuity equation and rearranging:

$$V_3 = \left[\frac{(V_1^3 + V_2^3 + V_4^3 + V_5^3)}{(V_1 + V_2 + V_4 + V_5)} \right]^{1/2} \tag{30}$$

Rearranging the continuity equation and substituting for V_3 from the preceding equation:

$$A_3 = A \left[\frac{(V_1 + V_2 + V_4 + V_5)^3}{(V_1^3 + V_2^3 + V_4^3 + V_5^3)} \right]^{1/2} \tag{31}$$

Next, substituting for A_3 and V_3 in the momentum equation:

$$A(P_1 - P_2 + P_4 - P_5) = \rho A (-V_1^2 + V_2^2 - V_4^2 + V_5^2)$$

$$- \rho A \left[\frac{(V_1 + V_2 + V_4 + V_5)^3}{(V_1^3 + V_2^3 + V_4^3 + V_5^3)} \right]^{1/2} \left[\frac{(V_1^3 + V_2^3 + V_4^3 + V_5^3)}{(V_1 + V_2 + V_4 + V_5)} \right] \cos \theta \tag{32}$$

Solving this equation for COS θ:

$$\cos \theta = \frac{\rho(- V_1^2 + V_2^2 - V_4^2 + V_5^2) - P_1 + P_2 - P_4 + P_5}{\rho \left[(V_1 + V_2 + V_4 + V_5)(V_1^3 + V_2^3 + V_4^3 + V_5^3) \right]^{1/2}} . \tag{33}$$

Finally, the expression for the angle of deflection which is comparable

to the experimental data is:

$$\phi = 90° - \cos^{-1}\left[\frac{\rho(-V_1^2 + V_2^2 - V_4^2 + V_5^2) - P_1 + P_2 - P_4 + P_5)}{\rho\left[(V_1 + V_2 + V_4 + V_5)(V_1^2 + V_2^2 + V_4^3 + V_5^3)\right]^{1/2}}\right] \quad (34)$$

A computer program was written using the preceding equation, the equations for flow in a slit, and the emperical equations for the control flow rates which would calculate the deflection angles, ϕ, for the entire control differential pressure range investigated experimentally for which $P_1 = P_2$ and $V_1 = V_2$. The program using the experimental nomenclature and the results are contained in Appendix B.

The jet interaction region investigated here was somewhat similar to the phenomena of the conventional jet beam deflection by transversely placed control jets. This had been investigated extensively, and recently an equation for the deflection angle was presented (13).

For jet beam deflection supply flow was introducted through a nozzle and formed the power jet, the direction of which could be modulated by introducing a control jet approximately perpendicular to the power jet. The additions of a second control jet opposite the first made possible the deflection of the power jet in a push-pull manner. The amount of this deflection was dependent on the differential control force, the tangent of the deflection angle being determined by dividing the sum of the pressure and momentum force differences in the two control ports by the total supply or power jet momentum; thus using the notation of Figure 13:

$$\tan\phi = \frac{P_5 A_5 - P_4 A_4 + (\rho/g)(A_5 V_5^2 - A_4 V_4^2)}{P_1 A_1 + P_2 A_2 + (\rho/g)(A_1 V_1^2 + A_2 V_2^2)} \quad (35)$$

where the supply flow exit area was equal to the sum of the exit areas of the channels which form the two wall jets. The resultant radial jet formed by the impacting wall jets replaced the power jet which was modulated by the control ports.

A computer program was written using the preceding equation, the equations for flow in a slit, and the emperical equations for the control flow rates which calculated the deflection angles, ϕ, for the entire control differential pressure range used for the control volume analysis and for the experimental investigation. This program and the results are contained in Appendix C.

New Configuration Analysis

The control volume method of analysis was applied to a new configuration which retained the impacting wall jets as the power supply jet but had the control ports placed perpendicular to the wall jets instead of parallel to them. It was felt that much larger deflection angles would be obtained from this configuration than from the previously discussed configuration, because the control signal would affect the impact plane, instead of deflecting a jet beam, which was the characteristic of the Direct Impact Modulator that gave it such high gains.

The additional assumptions in this analysis dealt with the geometrical arrangement of the control ports. It was assumed that $A_1 = A_2 = A_4 = A_5 = A$, the control ports were the same depth as the supply ports, the control ports were located at one control port width from the supply port exit and three port widths from the impact plane centerline, and pressure was applied only to the right control port which would deflect the resultant radial jet in the same direction as in the previous

investigations. These assumptions were applied as shown in Figure 14.

Control port flow characteristics were needed for this analysis; therefore, a reasonable assumption was made. From previous results it was known that

$$QCL = PCL/4.89 \text{ and } QCR = PCR/3.26;$$

an average of these would be a representative value for a channel which could be fabricated by the photo etching technique. This average was determined as,

$$QC = PC/4.08 \text{ and thus } QC = PC/4.0$$

was used for simplicity. Next, the control port length which was perpendicular to the wall jet was selected as one tenth of the length of the previous control port length which was parallel to the wall jet. For laminar flow in the control channel, this gave a control channel pressure drop equal to ten percent of that in the control channel of the previous configuration. With these assumptions the control port flow characteristic equation was,

$$QC = PC/40.0 \tag{36}$$

It was determined by computations that variations as large as an order of magnitude in this equation had negligible effects on the resultant jet deflection angles.

The jet beam deflection formula was used to determine the right wall jet deflection angle, α', since it had provided conservative results in comparison with experimental data that is, the calculated

deflection angles were less than experimentally determined deflection angles. Applying the jet beam deflection formula to the right side of the configuration shown in Figure 14 and in more detail in Figure 15 resulted in:

$$\tan \alpha' = \frac{P_5 A_5 + (\rho/g)\ (A_5 V_5^2)}{P_2 A_2 + (\rho/g)\ (A_2 V_2^2)} \tag{37}$$

where P_5 and P_2 were the gage pressures referred to atmospheric pressure P_o.

The deflection distance, Ds, through which the right supply wall jet was deflected in the y-direction as measured at the impact plane, ie. point B in Figure 15, was:

$$D_s = (4\ A_5 \tan \alpha')/d. \tag{38}$$

Now, the jets in this case did not impact completely with one another; they were off center by an amount D_s. The portion of the left wall jet flowing through the area, D_s by d, combined with the control flow. Since V_1 was much greater than V_5 and since it must be assumed that there was no wall jet flow into the control ports, no impact plane was formed by the portion of the wall jet momentum flux, $\rho\ V_1^2\ d\ D_s$, and the control jet with momentum flux, $\rho\ V_5^2\ A_5$. Rather, the control jet was entrained by the wall jet at a velocity V_1. At first the flux of this secondary jet was toward the point C in Figure 14.

At point C in Figure 15, the combined jet with an assumed cross sectional area of D_s by d flowing from left to right encountered the

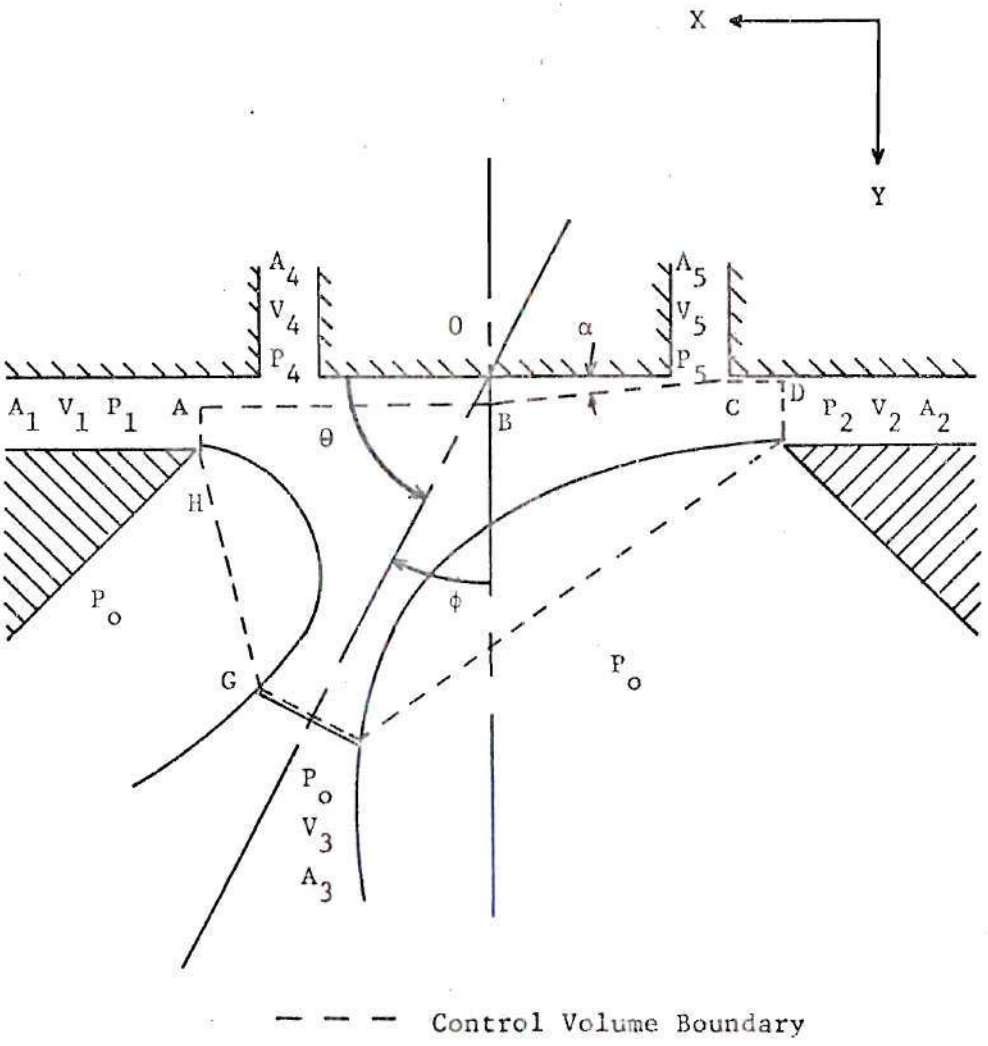

Figure 14. Impacting Wall Jets with Perpendicular Control Ports

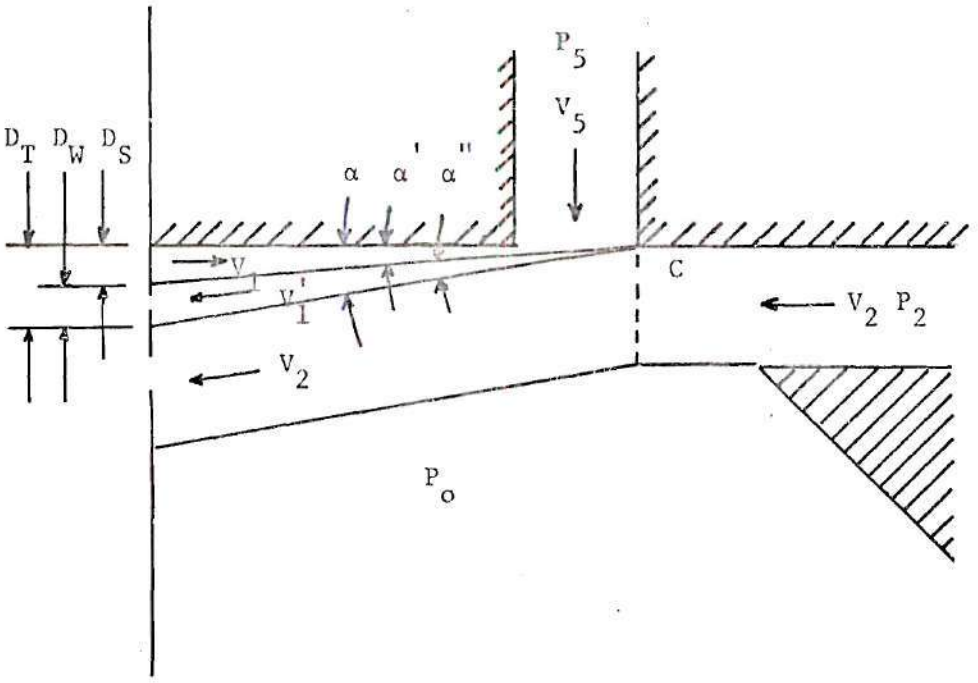

Figure 15. Deflection Angle Details

right wall jet with velocity V_2 flowing in the opposite direction. Since the velocities of the encountering jets were essentially the same, an impact region was formed which turned the combined jet through an angle of 180° - α, that is, the secondary impact caused a secondary deflection, α'', of the right wall jet over and above the original deflection α' previously determined. α was taken as the sum of α' and α''as shown in Figure 15. This secondary impact could be treated as equivalent to an additional control signal acting with a pressure of P_5 and with a velocity slightly less than V_1 on an area D_s by d.

As shown in Figure 15, D_w was the additional distance at the centerline impact plane when the right wall jet was deflected by an angle of α''. The portion of the left wall jet, which in combination with the right control flow formed a secondary jet, was entrained by the right wall jet; it was assumed that the additional width resulting from this entrainment was exactly equal to D_w as measured at the centerline impact plane. This was a reasonable assumption since the flow was considered incompressible and the calculations showed that α' and α'' were very nearly equal with α'' slightly greater than α'. Considering essentially equal velocities V_1, V_2 and V_1', the above indicated a stable impact phenomena within the region defined by D_w. An exact analysis should include the influences of viscous jet entrainment characteristics and velocity profiles. This is beyond the scope of the current investigation.

The total angle of deflection, α, through which the right wall jet was deflected could be given by:

$$\tan \alpha = \tan \alpha' + \frac{P_5 \; d \; D_s + (\rho/g) \; (d \; D_s \; V_1^2)}{P_2 \; A_2 + (\rho/g) \; (A_2 \; V_2^2)} \tag{39}$$

or substituting for $\tan \alpha'$, D_s, and the A's,

$$\tan \alpha = \frac{P_5 + (\rho/g) \; V_5^2 + (P_5 + (\rho/g) \; V_1^2) \; V_1^2) \quad 4.0 \tan \alpha'}{P_2 + (\rho/g) \; V_2^2} \tag{40}$$

and the total distance deflected as measured at the impact plane was given by:

$$D_T = D_s + D_w = (4.0 \; A \tan \alpha)/d \; . \tag{41}$$

Now referring to Figure 14, a control volume analysis was applied to the control volume ABCDEFGHA as outlined with a dashed line.

Applying the momentum theorem in the X-direction with $(P_o A_{GF})_X = (P_o A_{FE})_X$ and assuming $P_1 = P_2$ and $V_1 = V_2$:

$$- P_1 \; d \; \rho D_T = \quad V_1^2 \; d \; D_T - \; \rho A_3 \; V_3^2 \quad \cos \theta \; . \tag{42}$$

Applying the continuity equation:

$$2 \; V_1 \; A_1 + V_5 \; A_5 = A_3 \; V_3 \; . \tag{43}$$

Now, applying the energy equation and simplifying:

$$A \; (2 \; V_1^3 \; + V_5^3 \;) = A_3 \; V_3 \; V_3^2 \tag{44}$$

Substituting for $A_3 \; V_3$ from the continuity equation and rearranging:

$$V_3 = \left[\frac{2\ V_1^3 + V_5^3}{2\ V_1 + V_5} \right]^{1/2} \tag{45}$$

Rearranging the continuity equation and substituting for V_3 from the preceding equation:

$$A_3 = A \left[\frac{(2V_1 + V_5)^3}{2V_1^3 + V_5^3} \right]^{1/2} \tag{46}$$

Next, substituting for A_3, V_3, and D_T in the momentum equation:

$$\cos \theta = \frac{(P_1 + \rho V_1^2)\quad 4A \tan \alpha'}{\rho A \left[\frac{(2V_1 + V_5)^3}{(2V_1^3 + V_5^3)} \right]^{1/2} \left[\frac{2V_1^3 + V_5^3}{2\ V_1 + V_5} \right]} \tag{47}$$

finally,

$$\cos \theta = \frac{(4 \tan \alpha)(P_1 + \rho V_1^2)}{\rho \left[(2V_1^3 + V_5^3)(2V_1 + V_5) \right]^{1/2}} \tag{48}$$

A computer program was written using the preceding equation, the equations for flow in a slit, and the estimated equation for the control port pressure - flow characteristics. The program calculated the deflection angles, ϕ, for the entire control pressure range as was previously investigated. This program using the experimental nomenclature and the results of the program are contained in Appendix D.

CHAPTER V

DISCUSSION OF RESULTS

Jet Profiles

The resultant jet velocity profiles were well defined and exhibited all the the characteristics of a radial jet. In particular, the centerline velocity decreased almost linearly with increasing distance downstream from the impact region, and the jet demonstrated downstream spreading and entrainment which were viscous effects that were characteristic of all radial jets. Figure 10 shows the velocity decrease and the jet spreading while the total jet momentum remained essentially constant as represented by approximately equal area under each curve.

Parallel Control Configuration

The results are summarized in Table 3. The angles of deflection agreed within the experimental accuracy. If the boundary layer effects, the effect of entrainment from within the control volume, and the fact that the flow was more nearly three dimensional than two dimensional were taken into account, it would result in a decrease in the deflection angle for the control volume analysis. For these reasons and the fact that the difference in the overall deflection angle was only 2.70°, the experimental and the control volume results were considered in good agreement. The jet beam deflection calculations were in extremely close agreement with the experimental data differing by only 1.35°.

Table 3. Data Comparison for Transverse, Parallel Control Configuration

Pressure		PHI					
		Impact Configuration				Jet Beam	
PCR	PCR	Experimental		Control Volume		Deflection	
in. oil	in. oil	$\Delta\phi$	ϕ	$\Delta\phi$	ϕ	$\Delta\phi$	ϕ
3.2	3.2		2.78		.44		.23
		1.22		1.02		.45	
2.9	3.5		4.00		1.46		.68
		1.21		2.06		1.01	
2.3	4.1		5.21		3.52		1.69
		1.49		2.08		.81	
1.7	4.7		6.70		5.60		2.50
		.64		2.10		.94	
1.1	5.3		7.34		7.70		3.44
Overall $\Delta\phi$		4.56		7.26		3.21	

The impacting walls jets both with and without parallel control flow was a stable phenomena due primarily to the close proximity of the wall on one side and the cover plates on the other two sides. Further, in comparing the control volume analysis deflection angles with the jet beam deflection angles, the difference in the angles was due to the difference in Reynolds Number. The jet beam deflection angles were for flows with large Reynolds Numbers. The control volume analysis involved rather small Reynolds Numbers. Therefore, the viscous forces affect the deflection angles. If the viscous effects were taken into account, it would demonstrate the close agreement of the jet beam and the control volume analysis.

Perpendicular Control Configuration

A comparison of the analytical results of the transverse control configuration and the perpendicular control configuration is contained in Table 4. It can be seen that the deflection angles for the perpendicular configuration were approximately double those obtained for the transverse configuration. This will have a profoundly favorable effect on the operation of a fluidic amplifier which uses the impacting wall jets with perpendicular control flow to modulate the radial impact plane formed by two axially opposed impacting plane wall jets.

Table 4. Comparison of Control Volume Analysis

Control ΔP in. oil	Parallel Configuration		Perpendicular Configuration	
	ϕ	$\Delta\phi$	ϕ	$\Delta\phi$
0.0	0.44		0.0	
		1.02		2.08
0.6	1.46		2.08	
		2.06		4.41
1.8	3.52		6.49	
		2.08		4.75
3.0	5.60		11.24	
		2.10		5.14
4.2	7.70		16.38	
Overall $\Delta\phi$		7.26		16.38

CHAPTER VI

CONCLUSIONS

A fluidic device of the type represented by Configuration Number 8 proved to be unacceptable for use as a fluidic amplifier. Pressure gains were much lower than expected evidently due to the device operating as a jet beam deflection amplifier rather than operating as an impact modulator. Proper sizing and location of the output receivers of Configuration Number 8 would enable the device to approach the operating characteristics of a stream deflection amplifier which exhibit pressure gains of five to seven (14).

Impacting wall jets do, in fact, form a conventional radial jet which flows in a direction perpendicular to the flow direction of the wall jets. The modulation of this resultant radial jet by transversely placed control jets is described by jet beam deflection theory (13) which agrees with the control volume analysis presented in Chapter IV.

The control volume method is used to analyze placing the control ports perpendicular to the impacting wall jets. Applying a small positive control signal at one control port results in modulating the impact plane of the wall jets. This in turn results in a larger deflection angle for the radial jet. This modulation exhibits the characteristics of an impact modulator which have been shown to have large pressure gains when used as a fluidic amplifier (3). This perpendicular control port configuration is a very promising new configuration for use as a high gain

proportional fluidic amplifier.

One of the most outstanding contributions of this research is demonstrating the validity of using a relatively simple control volume analysis to determine the effects that various flows have on two impacting jets. This method would be valid for numerous investigations where a detailed analysis is not feasible and an overall approach would be satisfactory. Unfortunately this information has not been used extensively in the contemporary literature for fluidic device design.

CHAPTER VIII

RECOMMENDATIONS

A test device using perpendicular control ports similar to the configuration shown in Figure 14 should be constructed and tested in the same manner as described previously for measuring the velocity field of a radial jet with various control pressures. With this information the size and location of the output receivers for maximum pressure recovery and maximum pressure gain could be precisely determined. Combining these receivers with the impacting wall jets and the perpendicular control ports would result in a high gain proportional fluidic amplifier with stable operating characteristics since the analysis indicated stable impact phenomena. The control bias level should be very low, ie. sufficient to prevent flow into the control port. This should be determined by experiment.

Impacting wall jets offer many possibilities for further study. The difficulties involved in these studies should be more than compensated by the superior gains which show promise of developing from this type fluidic amplifier.

APPENDIX A

CALCULATIONS

The calculations required were programmed for the computer. The following calculations are representative of these computer calculations with the addition of checking the Reynolds Number of the flow in the supply and control channels. The nomenclature used is the same as that used for the computer programs.

Constants and the fluid properties are:

RHO = 0.00234 $lb_f sec^2/ft^4$

CMU = 0.000000375 lb_f sec/ft^2

C1 = 0.11069 in^3 hr in. oil/ft sec lb_f

C3 = 0.36138 lb_f/in. oil ft in.

C4 = 4.33653 lb_f/ft^2 in. oil

G = 0.23063 ft^2 in. oil/lb_f

$$PL = PS - \frac{3.0\ QS\ CMU\ SL}{2.0\ D\ B^3}\ C1$$

$$PL = 33.2 - \frac{(3.0)(5.0)(3.75 \times 10^{-7})(.28)}{(2.0)(.040)(.013)^3}\ (.11069)$$

$$PL = 33.2 - 0.99188$$

$$PL = 32.20812 \text{ in. oil}$$

$$VS \text{ average} = \frac{(PS - PL)B^2}{3.0\ CMU\ SL}\ C3$$

$$VS = \frac{(.99188)(6013)^2}{(3.0)(3.75 \times 10^{-7})(.28)}\ (.36138)$$

VS = 192.3076 ft/sec

QCL = PCL / 4.8932

QCL = 3.2 / 4.8932

QCL = 0.6540 CFH

QCR = PCR / 3.2621

QCR = 3.2 / 3.2621

QCR = 0.9810 CFH

$$P4 = PCL - \frac{3.0\ QCL\ CMU\ CL}{2.0\ D\ B^3}\ C1$$

$$P4 = 3.2 - \frac{(3.0)(.6540)(3.75 \times 10^{-7})\ .40}{(2.0)(.040)(.013)^3}\ (.11069)$$

P4 = 3.2 - 0.1853

P4 = 3.0147 in. oil

$$P5 = PCR - \frac{3.0\ QCR\ CMU\ CL}{2.0\ D\ B^3}\ C1$$

$$P5 = 3.2 - \frac{(3.0)(.9810)(3.75 \times 10^{-7})(.40)}{(2.0)(.040)(.013)^3}\ (.11069)$$

P5 = 3.2 - 0.2780

P5 = 2.9221 in. oil

$$VCL_{average} = \frac{(PCL - P4)\ B^2}{3.0\ CMU\ CL}\ C3$$

$$VCL = \frac{(.1853)(.013)^2}{(3.0)(3.75 \times 10^{-7})(.40)}\ (.36138)$$

VCL = 25.1526 ft/sec

$$VCR_{average} = \frac{(PCR - P5)\ B^2}{3.0\ CMU\ CL}\ C3$$

$$VCR = \frac{(.2780)(.013)^2}{(3.0)(3.75 \times 10^{-7})(.40)}\ (.36138)$$

VCR = 37.7293 ft/sec

$$R_e(VA) = \frac{RHO\ VA\ D}{CMU}$$

$$R_e = \frac{(.00234)(192.3076)(.026)}{3.75 \times 10^{-7}}$$

$$R_e = 2607.0$$

$$R_e(VCL) = \frac{RHO\ VCL\ D}{CMU}$$

$$R_e = \frac{(.00234)(25.1526)(.026)}{3.75 \times 10^{-7}}$$

$$R_e = 340.6$$

$$R_e(VCR) = \frac{RHO\ VCR\ D}{CMU}$$

$$R_e = \frac{(.00234)(25.1526)(.026)}{3.75 \times 10^{-7}}$$

$$R_e = 510.9$$

$$XIA = (2.0VS + VCL + VCR)^3$$

$$XIA = ((2.0)(192.3) + 25.15 + 37.73)^3$$

$$XIA = (447.49)^3$$

$$XIA = 89612869.58$$

$$XIB = 2.0VS^3 + VCL^3 + VCR^3$$

$$XIB = (2.0)(7112005.01) + (15911.74) + (53706.38)$$

$$XIB = 14293628.14$$

$$X2 = (XIA)^{1/3} \times IB$$

$$X2 = 6395908215.$$

$$X3 = VCR^2 - VCL^2$$

$X3 = 1423.47 - 632.62$

$X3 = 790.85$

$X4 = (P4 - P5)\ C4$

$X4 = (3.0157 - 2.9221)(4.33653)$

$X4 = 0.401381$

$$V3_{average} = \frac{XIB}{(XIA)^{1/3}}^{1/2}$$

$$V3 = \frac{14293628.14}{447.49}^{1/2}$$

$V3 = 178.72$

$$XCOS = \frac{RHO\ X3 + X4}{RHO\ (X2)^{1/2}}$$

$$XCOS = \frac{1.8506 + .401381}{187.14015}$$

$XCOS = 0.0120$

$PHI = COS^{-1}\ (XCOS)$

$PHI = 0.65$

APPENDIX B

COMPUTER PROGRAM AND RESULTS - TRANSVERSE JETS

The following is a listing of the computer program used to calculate the deflection angle, PHI, of the resultant radial jet formed by two impacting wall jets with parallel control channels. Table 5 contains the results of this computer program. This program is written in Fortran and was run on the Unavac 1108 computer.

```
      DIMENSION PCL(350)'PCR(350)
      RHO = 0.00234
      CMU = 0.000000375
      C1 = (12.0*27.687) / (3600.0*0.834)
      C3 = (0.834*12.0) / 27.684
      C4 = (0.834*144.0) / 27.684
      QS = 5.0
      SL = 0.28
      CL = 0.40
      B = 0.013
      D = 0.040
      PS = 33.2
      PL = (PS) - (3.0*QS*CMU*SL*C1) / (2.0*D*B**3)
      VSA = ((PS-PL)*C3*B**2) / (3.0*CMU*SL)
      WRITE(6'8) PS
    8 FORMAT (//'18H SUPPLY PRESSURE = 'F10.5'8H IN. OIL/)
      WRITE(6'9) QS
    9 FORMAT (14H SUPPLY FLOW = 'F10.5'4H CFH/)
      WRITE(6'10) PL
   10 FORMAT (26H SUPPLY EXIT PRESSURE'PL = 'F10.5'8H IN. OIL/)
      WRITE(6'11) VSA
   11 FORMAT (26H AVERAGE SUPPLY VELOCITY = 'F10.5'13H FT. PER SEC. //)
      WRITE(6'13)
   13 FORMAT(1X'119H   PCL(I)    PCR(I)    P4     P5      QCL
     X  QCR     VCL          VCR        V3A   XCOS    THETA    PHI
     X  /)
      WRITE(6'15)
   15 FORMAT (1X'119H   IN. OIL   IN.OIL    IN. OIL   IN. OIL    CFH
     X   CFH     FT/SEC     FT/SEC   FT/SEC              DEGREES  DEGRE
     XES//)
      PCL(1) = 3.2
      PCR(1) = 3.2
      DO 100 I=1'320
      QCL = PCL(I) / 4.893144
      QCR = PCR(I) / 3.262096
      P4 = (PCL(I)) - (3.0*QCL*CMU*CL*C1) / (2.0*D*B**3)
      P5 = (PCR(I)) - (3.0*QCR*CMU*CL*C1) / (2.0*D*B**3)
      VCL = ((PCL(I) - P4)*C3*N**2) / (3.0*CMU*CL)
      VCR = ((PCR(I) - P5)*C3*b**2) / (3.0*CMU*CL)
      V3A = SQRT((2.0*VSA**3 + VCL **3 + VCR**3) / (2.0*VSA + VCL +
     X VCR)
      X2 = (2.0*VDA + VCL + VCR)*(2.0*VSA**3 + VCL**3 + VCR**3)
      X3 = VCR**2 - VCL**2
      X4 = (P5-P4)*C4
      XCOS = (RH)*X3+X4) / (RHO*SQRT(X2))
      THETA = (180.0*ACOS(XCOS)) / 3.14159
      PHI = 90.0 - THETA
      WRITE(6.14) PCL(I)'PCR(I)'P4'P5'QCL'QCR'VCL/VCR'V3A'XCOS'THETA'P
     XHI
   14 FORMAT(12F10.5)
```

```
      PCL(I+1) = PCL(I) - 0.01
      PCR(I+1) = PCR(I) + 0.01
100   CONTINUE
      END
```

Table 5. Computer Program Results

Data Point	1	2	3	4	5
PCL(I)	3.2000	2.9000	2.3000	1.7000	1.1000
PCR(I)	3.2000	3.5000	4.1000	4.7000	5.3000
P4	3.0147	2.7321	2.1668	1.6016	1.0363
P5	2.9221	3.1960	3.7439	4.2918	4.8397
QCL	.6540	.5927	.4700	.3474	.2248
QCR	.9810	1.0729	1.2569	1.4408	1.6247
VCL	25.155	22.797	18.081	13.364	8.647
VCR	37.733	41.271	48.346	55.421	62.496
V3A	178.74	178.58	178.34	178.21	178.19
XCOS	.0074	.02550	.06133	.09752	.13398
THETA	89.556	88.539	86.484	84.404	82.300
PHI	.4435	1.4613	3.5163	5.5961	7.6995

Supply Pressure = 33.20 in. oil

Supply Flow = 5.00 CFH

Supply Exit Pressure, PL = 32.084 in. oil

Average Supply Velocity = 192.33 ft/sec

APPENDIX C

COMPUTER PROGRAM AND

RESULTS -- JET BEAM DEFLECTION

The following is a listing of the computer program used to calculate the deflection angle, PHI, of jet with an exit area equal to the sum of the exit areas of the supply channels of the wall jet configuration device which is modulated with transversely placed control jets. Table 6 contains the results of this computer program. This program is written in Fortran and was run on the Unavac 1108 computer.

```
   DIMENSION PCL(350)'PCR(350)
   RHO = 0.00234
   CMU = 0.000000375
   C1 = (12.0*27.687) / (3600.0*0.834)
   C3 = (0.834*12.0) / 27.684
   QS = 5.0
   SL = 0.28
   CL = 0.40
   B = 0.013
   D = 0.040
   PS = 33.2
   G = 407.0 / (0.834*2116.0)
   PL = (PS) - (3.0*QS*CMU*SL*C1) / (2.0*D*B**3)
   VSA = ((PS-PL)*C3*B**2)/(3.0*CMU*SL)
   WRITE(6'8) PS
 8 FORMAT (//'18H SUPPLY PRESSURE ='F10.5'8H IN.OIL/)
   WRITE(6'9) QS
 9 FORMAT (14H SUPPLY FLOW ='F10.5'4H CFH/)
   WRITE(6'10) PL
10 FORMAT (26H SUPPLY EXIT PRESSURE'PL = 'F10.5'8H IN. OIL/)
   WRITE(6'13)
13 FORMAT(1X'119H   PCL(I)    PCR(I)    P4       P5        QCL
  X  QCR      VACL       VACR        V3A     XTAN      THETA      PHI
  X  /)
   WRITE(6'15)
15 FORMAT (1X'119H IN.OIL     IN. OIL   IN. OIL    IN. OIL      CFH
  X   CFH       FT?SEC  FT?SEC     FT?SEC              DEGREES    DEGRE
  XES//)
   PCL(1) = 3.2
   PCR(1) = 3.2
   D) 100 I = 1'320
   QCL = PCL(I) / 4.893144
   QCR = PCR(I) / 3.262096
   P4 = (PCL(I)) - (3.0*QCL*CMU*CL*C1) / (2.0*D*B**3)
   P5 = (PCR(I)) - (3.0*QCR*CMU*CL*C1) / (2.0*D*B**3)
   VCAL = ((PCL(I) - P4)*C3*B**2) / (3.0*CMU*CL)
   VCAR = ((PCR(I) - P5)*C3*B**2) / (3.0*CMU*CL)
   V3A = SQRT((2.0*VSA**3 + VCAL**3 + VCAR**3) / (2.0*VSA + VCAL +
  X VCAR))
   X6 = PCR(I) - PCL(I)
   X7 = RHO*G*(VCAR**2-VCAL**2)
   X8 = 2.0*(PL + RHO*G*VSA**2)
   XTAN = (X6+X7) / X8
   THETA = ATAN(XTAN)
   PHI = (180.0*THETA) / 3.14159
   THETA = 90.0 - PHI
   WRITE(6'14) PCL(I)'PCR(I)'P4'(P'QCL'QCR'VCAL'VCAR'V3A'XTAN'THETA'P
  XHI
14 FORMAT(12F10.5
   PCL(I+1) = PCL(I) - 0.01
```

```
      PCR(I+1) = PCR(I) + 0.01
100   CONTINUE
      END
```

Table 6. Computer Program Results

Data Point	1	2	3	4	5
PCL(I)	3.2000	2.9000	2.3000	1.7000	1.1000
PCR(I)	3.2000	3.5000	4.1000	4.7000	5.3000
P4	3.0147	2.7321	2.1668	1.6016	1.0363
P5	2.9221	3.1960	3.7439	4.2918	4.8397
QCL	.6540	.5927	.4700	.3474	.2248
QCR	.9810	1.0729	1.2569	1.4408	1.6247
VCL	25.156	22.797	18.081	13.364	8.6473
VCR	37.733	41.271	48.346	55.421	62.496
V3A	178.74	178.58	178.34	178.21	178.19
XTAN	.00409	.01187	.02765	.04371	.06007
THETA	89.766	89.319	88.416	87.497	86.563
PHI	.2344	.6802	1.5838	2.5030	3.4374

Supply Pressure = 33.20 in. oil

Supply Flow = 5.00 CFH

Supply Exit Pressure, PL = 32.2084 in. oil

Average Supply Velocity = 192.33 ft/sec

APPENDIX D

COMPUTER PROGRAM AND

RESULTS - PERPENDICULAR JETS

The following is a listing of the computer program used to calculate the deflection angle, PHI, of the resultant radial jet formed by two impacting wall jets which is modulated by a control jet placed perpendicular to the right wall jet. Table 7 contains the results of this computer program. This program is written in Fortran and was run on the Univac 1108 computer.

```
      DIMENSION PCI(500)
      RHO = 0.00234
      CMU = 0.000000375
      C1 = (12.0*27.687) / (3600.0*0.834)
      C3 = (0.834*12.0) / 27.684
      QS = 5.0
      SL = 0.28
      CL = 0.040
      W = 0.026
      B = 0.013
      D = 0.040
      PS = 33.2
      G = 407.0 / (0.834*2116.0)
      PL = (PS) - (3.0*QS*CMU*SL*C1) / (2.0*D*B**3)
      VS = ((PS-PL)*C3*B**2) / (3.0*CMU*SL)
      WROTE(6'8)PS
    8 FORMAT (//'18H SUPPLY PRESSURE = 'F10.5'8H IN. OIL/)
      WRITE(6'9) QS
    9 FORMAT (14H SUPPLY FLOW = 'F10.5'4H CFH/)
      WRITE(6/10) PL
   10 FORMAT (26H SUPPLY EXIT PRESSURE'PL = 'F10.5'8H IN. OIL/)
      WRITE(6/11) VS
   11 FORMAT (26H AVERAGE SUPPLY VELOCITY = 'F10.5'13H FT. PER SEC.//).
      WRITE(6'13)
   13 FORMAT(100H   PCI(I)     PC       QC      VC       XTAN     ALP
     XHA       DT        V3       XCOS      PHI /)
      WRITE(6'15)
   15 FORMAT(100H  IN. OIL     IN. OIL     CFH       FT/SEC       DEG
     XREES      IN       FT/SEC                DEGREES  //)
      PCI(I) = 0.0
      DO 100 I = 1'500
      QC = PCI(I) /40.0
      PC = PCI(I) - (3.0*QC*CMU*CL*C1) / (80.0*D*B**3)
      VC = ((PCI(I) - PC)*C3*B**2) / (3.0*CMU*CL)
      XTAN = (PC + RHO*G*VC**2) / (PL + RHO*G*VS**2)
      B1 = PC + RHO*G*VC**2
      B2 = PL + RHO*G*VS**2
      B3 = PC*4.0*XT_N + RHO*G*4.0*XTAN*VS**2
      XTAN = (B1 + B3) / B2
      ALPHA = ATAM(XTAN)
      ALPHA = (180.0*ALPHA) / 3.14159
      DT = 4.0*W*XTAN
      X1 = RHO*(SQRT((2.0*VS**3 + VC**3) * (2.0*VS + VC)))
      X2 = (XTAN*(PS + RHO*G*VS**2))
      XCOS = 4.0*X27X1
      THETA = ACOS(XCOS)
      PHI = 90.0 - ((180.0*THETA) / 3.14159
      V3 = SQRT((2.0*VS**3 + VC**3) / (2.0*VS + VC))
      WRITE(6'14) PCI(I)'PC'QC'VC'XTAN'ALPHA'DT'V3'XCOS'PHI
   14 FORMAT(6F10.6'1X'F10.9'1X'3F10.6)
      PCI(I+1) = PCI(I) + 0.010000
  100 CONTINUE
      END
```

Table 7. Computer Program Results

Data Point	1	2	3	4	5
PCI(I)	0.0000	.6000	1.8000	3.0000	4.2000
PC	0.0000	.5999	1.7999	2.9999	4.1999
QC	0.0000	.0150	.0450	.0750	.1050
VC	0.0000	.0144	.0433	.0721	.1009
XTAN	0.0000	.0296	.0921	.1587	.2296
ALPHA	0.0000	1.6973	5.2603	9.0198	12.9332
DT	0.0000	.00308	.00957	.01651	.02388
V3	192.33	192.32	192.32	192.31	192.30
XCOS	0.0000	.0363	.1131	.1949	.2820
PHI	0.0000	2.0858	6.4933	11.2431	16.3824

Supply Pressure = 33.20 in. oil

Supply Flow = 5.00 CFH

Supply Exit Pressure, PL = 32.21 in. oil

Average Supply Velocity = 192.33 ft/sec

APPENDIX E

SCHEMATICS

Following in Figures 16 and 17 are the construction details for the test amplifier, Configuration Number 8 and the test device for velocity field measurements. Figure 18 is a list of symbols used in Figures 19 and 20 which are the schematics for the test system for the fluidic amplifier and for the test system for the velocity profile studies respectively.

Notes: (1) Channel widths = .026"

(2) Radius of curvature small = .140"
large = .306"

(3) Overall dimensions 4 inches square

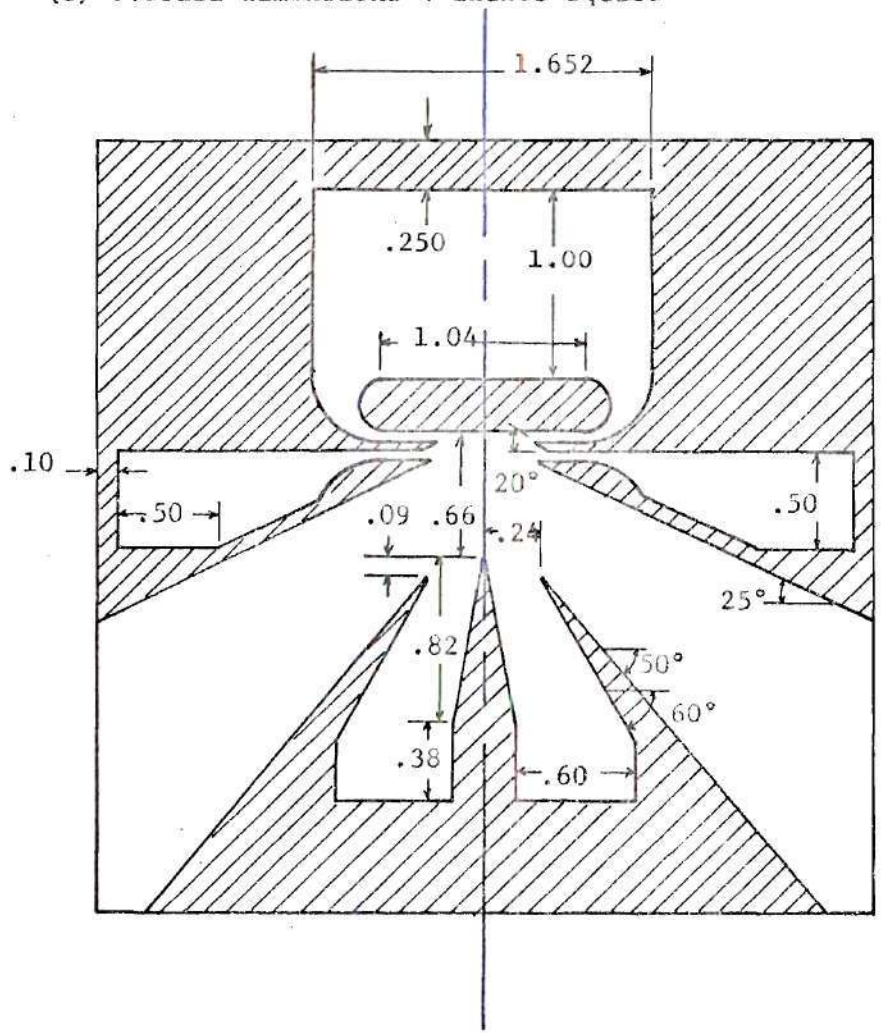

Figure 16. Test Amplifier Details

Notes: (1) Channel widths = .026"

(2) Radius of curvature small = .140"
large = .306"

(3) Overall dimensions 4 inches square

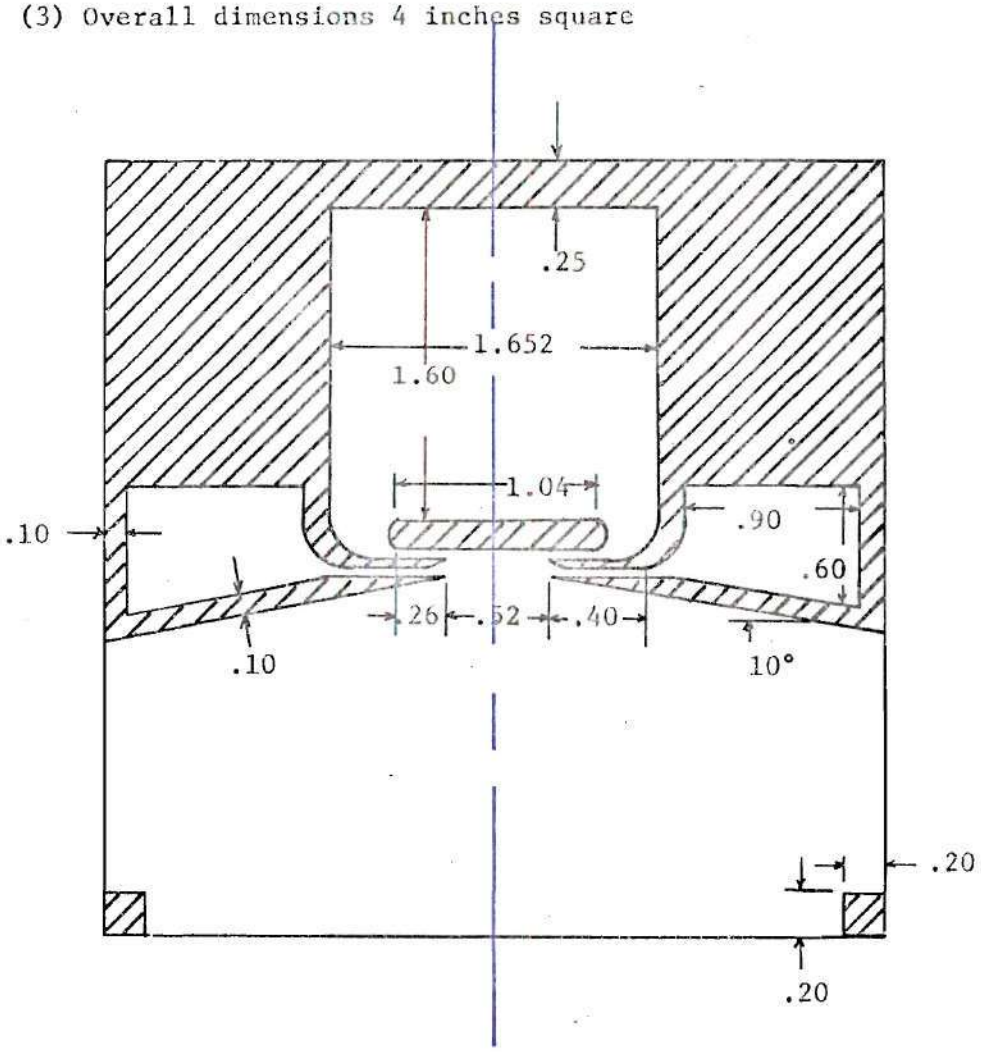

Figure 17. Test Device Details

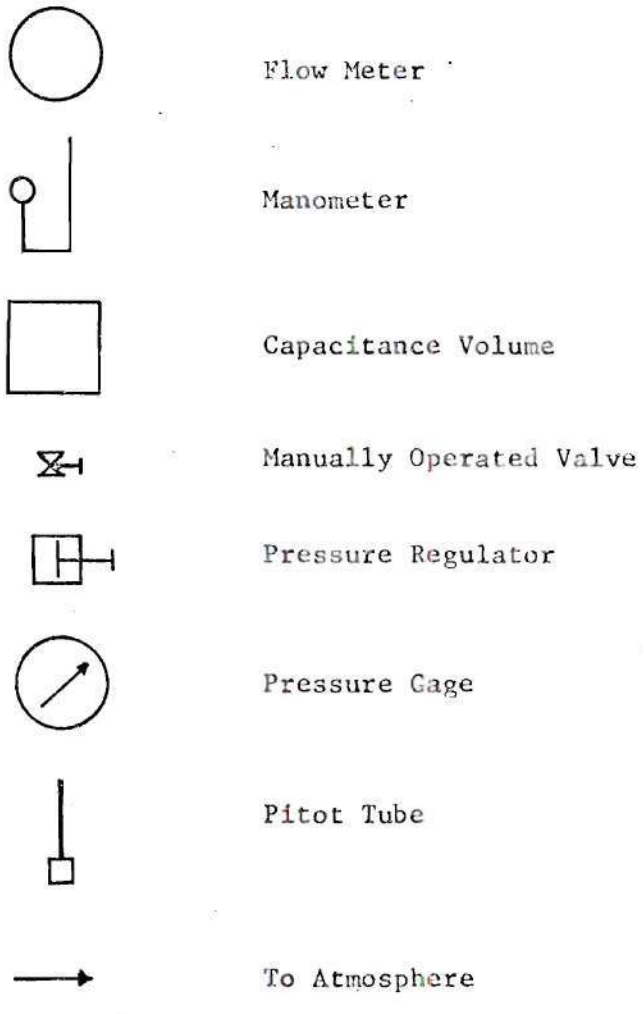

Figure 18. Schematic Symbols

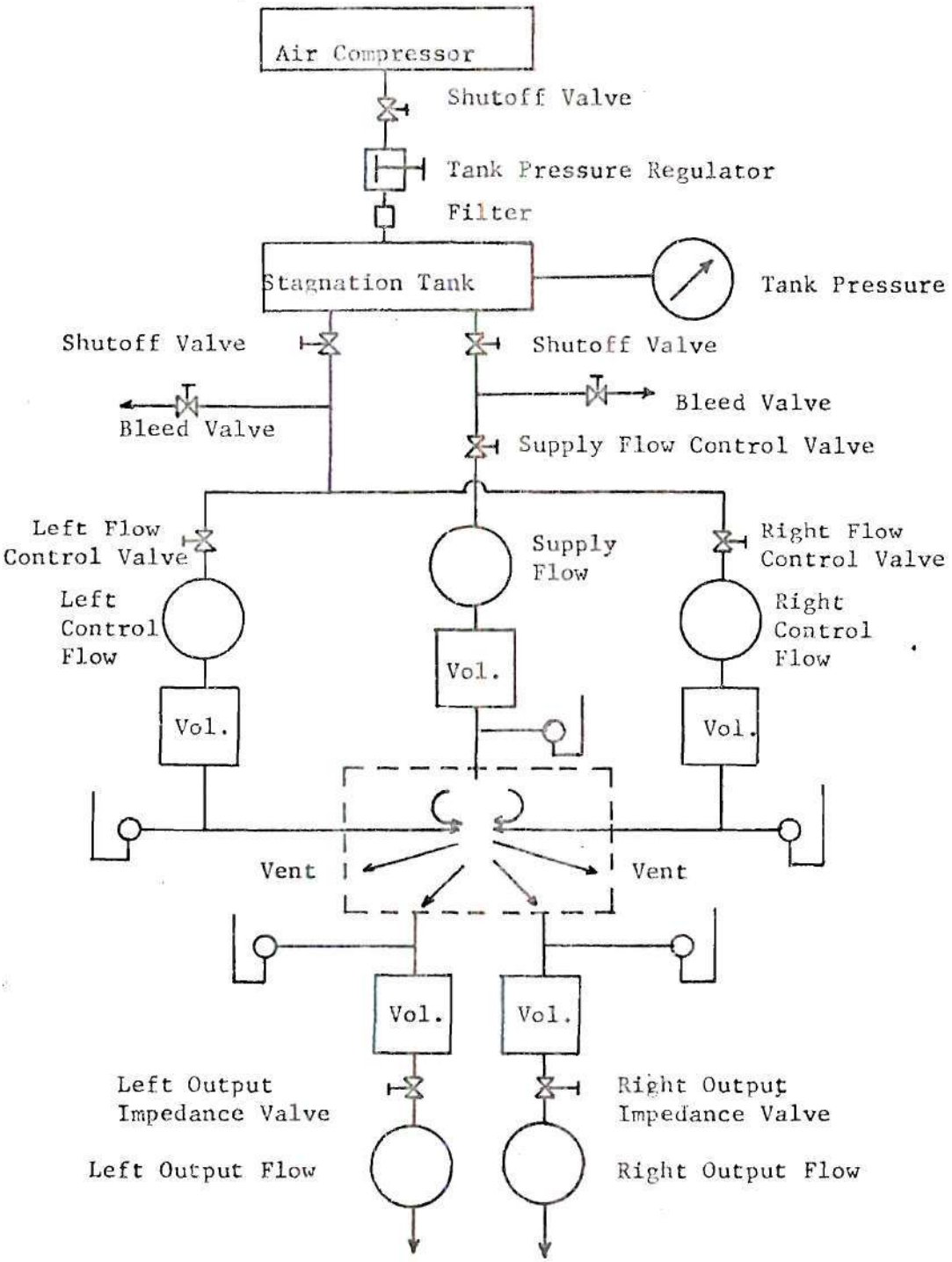

Figure 19. Test System Schematic for Fluidic Amplifier

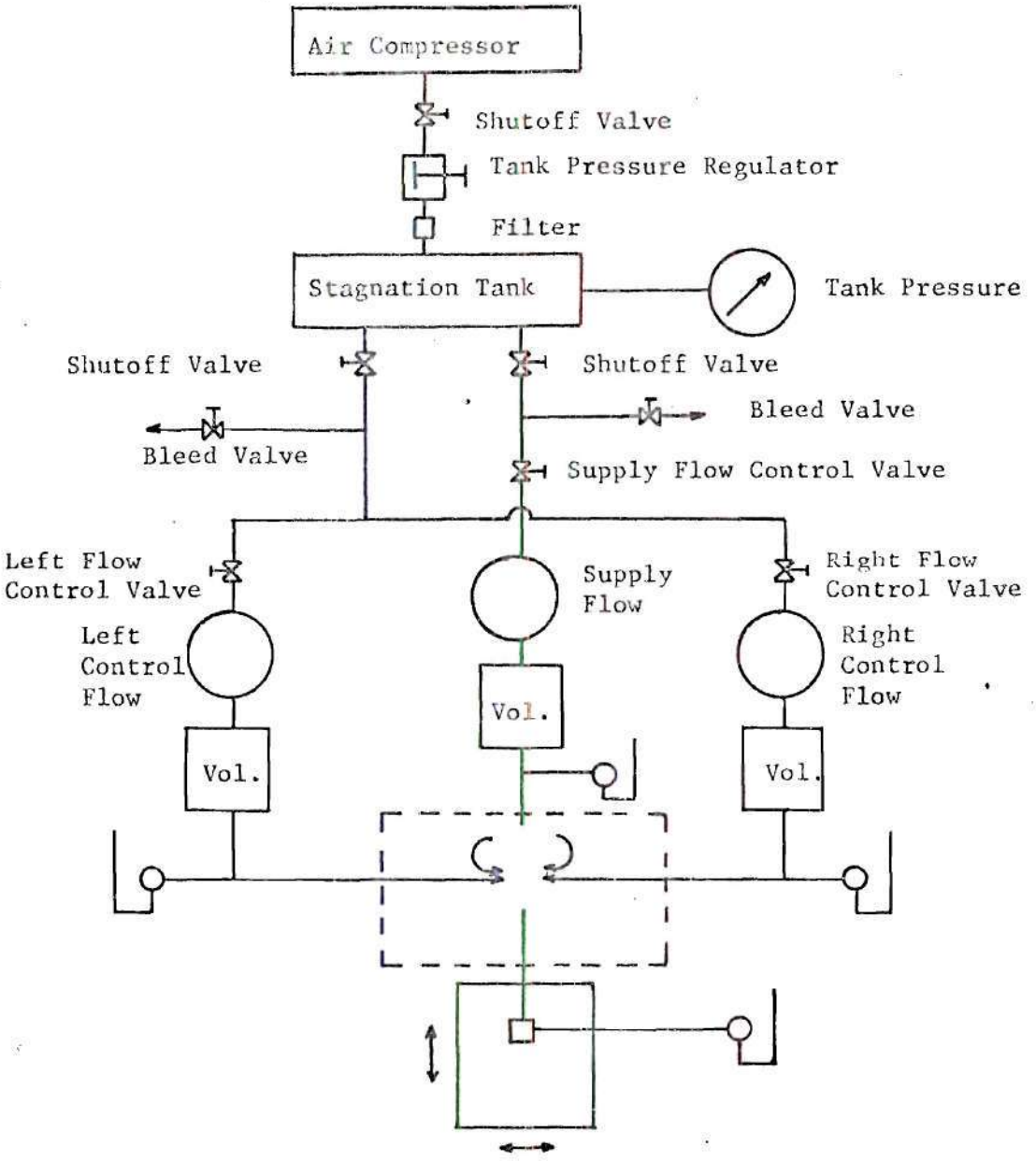

Figure 20. Test System Schematic for Velocity Profile Studies

APPENDIX F

DATA

Following in Tables 8, 9, 10, 11, 12, 13, 14, 15, 16, and 17 are the rough data used in developing the graphs and tables in this investigation.

Table 8. Configuration Number 8 Data

Configuration Number 8

Output Impedance Minimum

Bias Level 5.0%

Supply		Control				Output			
		Left		Right		Left		Right	
Press in. Hg	Flow CFH	Press in. oil	Flow CFH	Press in. oil	Flow CFH	Press in. oil	Flow CFH	Press in. oil	Flow CFH
2.0	8.40	1.5	0.0	1.5	0.0	1.0	0.0	2.2	2.4
2.0	8.40	1.0	0.0	2.0	0.0	1.3	0.0	2.4	2.3
2.0	8.40	0.5	0.0	2.5	0.0	1.5	0.5	2.3	2.2
2.0	8.40	0.0	0.0	3.0	0.0	1.8	0.9	2.0	2.1
2.0	8.40	1.5	0.0	1.5	0.0	1.0	0.0	2.3	2.4
2.0	8.40	2.0	0.0	1.0	0.0	0.6	0.0	2.2	2.3
2.0	8.40	2.5	0.0	0.5	0.0	0.3	0.0	2.0	2.1

Note: Control flows were below the range of the control flow meters.

Table 9. Configuration Number 8 Data

Configuration Number 8

Output Impedance Minimum

Bias Levely 10.0%

Supply		Control				Output			
		Left		Right		Left		Right	
Press in. Hg	Flow CFH	Press in.oil	Flow CFH	Press in.oil	Flow CFH	Press in.oil	Flow CFH	Press in.oil	Flow CFH
2.0	8.40	3.0	0.0	3.0	0.0	1.1	0.0	2.4	2.5
2.0	8.40	2.5	0.0	3.5	0.0	1.4	0.0	2.4	2.5
2.0	8.40	2.0	0.0	4.0	0.0	1.6	0.7	2.4	2.5
2.0	8.40	1.5	0.0	4.5	0.0	2.0	1.0	2.4	2.5
2.0	8.40	1.0	0.0	5.0	0.0	2.1	1.4	2.1	2.1
2.0	8.40	0.5	0.0	5.5	0.0	2.3	1.5	2.0	2.0
2.0	8.40	0.0	0.0	6.0	0.0	2.5	1.7	1.6	1.9
2.0	8.40	3.0	0.0	3.0	0.0	1.1	0.0	2.4	2.5
2.0	8.40	3.5	0.0	2.5	0.0	0.8	0.0	2.3	2.4
2.0	8.40	4.0	0.0	2.0	0.0	0.5	0.0	2.1	2.1
2.0	8.40	4.5	0.0	1.5	0.0	0.2	0.0	2.0	2.0
2.0	8.40	5.0	0.0	1.0	0.0	0.0	0.0	1.8	2.0

Note: Control flows were below the range of the control flow meters.

Table 10. Configuration Number 8 Data

Configuration Number 8

Output Impedance Minimum

Bias Level 12.5%

Supply		Control				Output			
		Left		Right		Left		Right	
Press in. Hg	Flow CFH	Press in.oil	Flow CFH	Press in.oil	Flow CFH	Press in.oil	Flow CFH	Press in.oil	Flow CFH
2.0	8.40	4.1	0.0	4.1	0.0	1.1	0.0	2.5	2.9
2.0	8.40	3.2	0.0	5.0	0.0	1.5	0.6	2.4	2.8
2.0	8.40	2.2	0.0	6.0	0.0	2.0	1.3	2.2	2.5
2.0	8.40	1.2	0.0	7.0	0.0	2.45	1.5	2.0	2.2
2.0	8.40	0.2	0.0	8.0	0.0	2.7	1.8	1.8	2.0
2.0	8.40	-0.3	0.0	8.5	0.0	2.7	1.9	1.5	1.8
2.0	8.40	4.1	0.0	4.1	0.0	1.1	0.0	2.5	2.9
2.0	8.40	5.2	0.0	3.0	0.0	0.5	0.0	2.1	2.1
2.0	8.40	6.0	0.0	2.2	0.0	0.0	0.0	1.9	2.0

Note: Control flows were below the range of the control flow meters.

Table 11. Configuration Number 8 Data

Configuration Number 8

Output Impedance Minimum

Bias Level 23.0%

Supply		Control				Output			
		Left		Right		Left		Right	
Press	Flow	Press	Flow	Press	Flow	Press	Flow	Press	Flow
in. Hg	CFH	in.oil	CFH	in.oil	CFH	in.oil	CFH	in.oil	CFH
2.0	8.40	5.2	0.0	10.0	0.0	2.6	1.7	2.4	2.6
2.0	8.40	6.2	0.0	9.0	0.0	2.1	1.4	2.6	3.0
2.0	8.40	7.2	0.0	8.0	0.0	1.6	0.7	2.8	3.1
2.0	8.40	8.2	0.0	7.0	0.0	1.2	0.0	2.6	3.1
2.0	8.40	9.2	0.0	6.0	0.0	0.5	0.0	2.4	3.0

Note: Control flows were below the range of the control flow meters.

Table 12. Velocity Field Data

P_s = 1 psi

Q_s = 10 CFH

Control Bias Level 10%

Left; Right
3.2 in. oil; 3.2 in. oil

Position	0.9	0.8	0.7	0.6	0.5	0.4	0.3	0.2	0.1	℄
0.0										
0.1										
0.1	0.044	edge							-0.30	4.40
0.2	0.074	edge							-0.15	4.40
0.3	0.108	edge						-0.15	0.25	4.00
0.4	0.130	edge						-0.15	0.45	3.60
0.5	0.145	edge						-0.15	0.70	3.20
0.6	0.180	edge						-0.10	0.90	2.60
0.7	0.200	edge						0.0	1.00	2.30
0.8	0.233	edge					-0.05	0.15	1.05	2.05
0.9										
0.9	0.250	edge					-0.05	0.30	1.07	1.80
1.0	0.280	edge					0.01	0.35	1.10	1.60
1.1	0.325	edge				0.0	0.03	0.40	1.00	1.30
1.2	0.350	edge				0.0	0.05	0.45	0.95	1.15
1.3	0.400	edge			0.0	0.01	0.10	0.48	0.85	1.05
1.4	0.510	edge		0.0	0.01	0.05	0.13	0.50	0.80	0.90
1.5	0.625	edge		0.01	0.01	0.07	0.15	0.50	0.70	0.80
1.6	0.655	edge	0.0	0.01	0.01	0.08	0.17	0.45	0.60	0.65
1.7	0.800	0.0	0.01	0.01	0.02	0.07	0.20	0.40	0.50	0.55

Table 12. Velocity Field Data (continued)

P_s = 1 psi Control Bias Level 10%

Q_s = 10 CFH Left ; Right
3.2 in. oil; 3.2 in. oil

℄	0.1	0.2	0.3	0.4	0.5	0.6	0.7	0.8	0.9	Position
										0.0
(Maximum 6.90 in. oil at right 0.038 inches)										0.1
4.40	4.00	-0.30						0.140	edge	0.1
4.40	2.90	-0.20						0.155	edge	0.2
4.00	2.80	-0.15						0.175	edge	0.3
3.60	2.30	-0.10						0.187	edge	0.4
3.20	1.80	-0.01						0.190	edge	0.5
2.60	1.40	0.0						0.20	edge	0.6
2.30	1.35	0.10	-0.10					0.211	edge	0.7
2.05	1.15	0.10	-0.05					0.234	edge	0.8
(Maximum 1.81 in. oil at left 0.008 inches)										0.9
1.80	1.00	0.10	-0.05					0.250	edge	0.9
1.60	0.95	0.10	0.0					0.255	edge	1.0
1.30	0.70	0.10	0.0					0.265	edge	1.1
1.15	0.60	0.15	0.01	0.0				0.300	edge	1.2
1.05	0.58	0.17	0.01	0.0				0.360	edge	1.3
0.90	0.55	0.20	0.07	0.01	0.0			0.425	edge	1.4
0.80	0.50	0.21	0.08	0.01	0.01	0.0		0.510	edge	1.5
0.65	0.45	0.22	0.08	0.01	0.01	0.0		0.625	edge	1.6
0.55	0.40	0.21	0.08	0.01	0.01	0.01	0.0	0.800	edge	1.7

Table 13. Velocity Field Data

P_s = 1 psi Control Bias Level 10%

Q_s = 10 CFH Left; Right
2.9 in. oil; 3.5 in. oil

Position	0.9	0.8	0.7	0.6	0.5	0.4	0.3	0.2	0.1	¢
0.0	0.023	edge							-0.45	2.50
0.1										
0.1	0.055	edge							-0.40	4.20
0.2	0.80	edge							-0.20	4.10
0.3	0.110	edge						-0.20	0.15	3.70
0.4	0.125	edge						-0.20	0.40	3.30
0.5	0.148	edge						-0.15	0.70	2.90
0.6	0.178	edge						-0.10	0.80	2.60
0.7	0.207	edge					-0.10	0.10	1.00	2.25
0.8	0.236	edge					-0.10	0.15	1.20	2.00
0.9	0.358	edge					-0.05	0.25	1.20	1.75
0.9										
1.0										
1.1	0.310	edge				0.0	0.01	0.38	1.20	1.43
1.2	0.325	edge				0.0	0.03	0.45	1.10	1.25
1.3	0.410	edge			0.0	0.01	0.10	0.52	1.05	1.13
1.4	0.525	edge		0.0	0.01	0.01	0.17	0.52	1.00	1.00
1.5	0.700	edge	0.0	0.01	0.01	0.01	0.20	0.52	0.90	0.90
1.6	0.900	edge	0.01	0.01	0.01	0.03	0.21	0.50	0.70	0.70
1.7	0.01	0.01	0.01	0.01	0.02	0.05	0.23	0.45	0.65	0.60

Table 13. Velocity Field Data (continued)

P_s = 1 psi Control Bias Level 10%

Q_s = 10 CFH Left ; Right
2.9 in oil; 3.5 in. oil

℄	0.1	0.2	0.3	0.4	0.5	0.6	0.7	0.8	0.9	Position
2.50										0.0
(Maximum 6.70 in. oil at right 0.038 inches)										0.1
4.20	4.30	-0.30						0.168	edge	0.1
4.10	2.90	-0.20						0.170	edge	0.2
3.70	2.20	-0.20						0.175	edge	0.3
3.30	1.75	-0.10						0.178	edge	0.4
2.90	1.50	-0.05						0.180	edge	0.5
2.60	1.20	0.0						0.200	edge	0.6
2.25	1.10	0.05						0.215	edge	0.7
2.00	0.90	0.07						0.225	edge	0.8
1.75	0.85	0.10	-0.05					0.238	edge	0.9
(Maximum 1.80 in. oil at left 0.018 inches)										0.9
										1.0
1.43	0.70	0.10	0.0					0.240	edge	1.1
1.25	0.65	0.15	0.01					0.300	edge	1.2
1.13	0.63	0.18	0.01	0.0				0.350	edge	1.3
1.00	0.60	0.20	0.01	0.01				0.560	edge	1.4
0.90	0.50	0.20	0.01	0.01				0.630	edge	1.5
0.70	0.45	0.20	0.02	0.01				0.760	edge	1.6
0.60	0.40	0.20	0.03	0.01				0.900	edge	1.7

Table 14. Velocity Field Data

P_s = 1 psi

Q_s = 10 CFH

Control Bias Level 10%

Left; Right
2.3 in. oil; 4.1 in. oil

Position	0.9	0.8	0.7	0.6	0.5	0.4	0.3	0.2	0.1	℄
0.0										
0.1										
0.1	0.048	edge							-0.40	4.70
0.2	0.089	edge							-0.20	4.50
0.3	0.109	edge						-0.20	0.30	4.00
0.4	0.139	edge						-0.15	0.50	3.50
0.5	0.168	edge						-0.10	0.95	3.05
0.6	0.189	edge						-0.05	1.10	2.65
0.7	0.224	edge						0.10	1.20	2.30
0.8	0.248	edge					-0.10	0.20	1.35	2.00
0.9	0.283	edge					-0.01	0.40	1.30	1.65
0.9										
1.0										
1.1	0.325	edge				0.0	0.01	0.40	1.10	1.20
1.2	0.360	edge				0.0	0.05	0.45	1.00	1.00
1.3	0.400	edge			0.0	0.01	0.10	0.50	0.90	0.90
1.4	0.450	edge			0.0	0.01	0.15	0.50	0.80	0.72
1.5	0.59	edge		0.0	0.01	0.01	0.20	0.50	0.75	0.65
1.6	0.730	edge	0.01	0.01	0.01	0.05	0.22	0.48	0.70	0.58
1.7	0.70	edge	0.01	0.01	0.01	0.10	0.25	0.45	0.60	0.52

Table 14. Velocity Field Data (continued)

P_s = 1 psi Control Bias Level 10%

Q_s = 10 CFH Left; Right
2.3 in. oil; 4.1 in. oil

℄	0.1	0.2	0.3	0.4	0.5	0.6	0.7	0.8	0.9	Position
										0.0
(Maximum 6.80 in. oil at right 0.038 inches)										0.1
4.70	4.10	-0.25						0.140	edge	0.1
4.50	2.70	-0.20						0.150	edge	0.2
4.00	2.10	-0.15						0.165	edge	0.3
3.50	1.60	-0.10						0.175	edge	0.4
3.05	1.30	-0.10						0.178	edge	0.5
2.65	1.05	-0.03						0.163	edge	0.6
2.30	0.90	-0.01						0.189	edge	0.7
2.00	0.70	0.03	-0.01					0.214	edge	0.8
1.65	0.70	0.05	-0.05					0.231	edge	0.9
(Maximum 1.80 in. oil at left 0.035 inches)										0.9
1.20	0.60	0.05	0.0					0.250	edge	1.1
1.00	0.50	0.05	0.0					0.275	edge	1.2
0.90	0.45	0.07	0.01	0.0				0.300	edge	1.3
0.72	0.40	0.10	0.01	0.0				0.345	edge	1.4
0.65	0.40	0.10	0.02	0.01	0.01			0.523	edge	1.5
0.58	0.35	0.10	0.02	0.01	0.01	0.01		0.652	edge	1.6
0.52	0.32	0.12	0.03	0.02	0.02	0.01	0.01	0.840	edge	1.7

Table 15. Velocity Field Data

P_s = 1 psi

Q_s = 10 CFH

Control Bias Level 10%

Left; Right
1.7 in. oil; 4.7 in. oil

Position	0.9	0.8	0.7	0.6	0.5	0.4	0.3	0.2	0.1	¢
0.0										
0.1										
0.1	0.056	edge							-0.40	5.10
0.2	0.088	edge							-0.35	4.80
0.3	0.117	edge						-0.20	0.45	4.25
0.4	0.146	edge						-0.15	0.70	3.70
0.5	0.175	edge						-0.10	1.15	3.15
0.6	0.206	edge					-0.15	0.02	1.40	2.65
0.7	0.232	edge					-0.10	0.20	1.55	2.20
0.8	0.270	edge					-0.10	0.40	1.60	1.80
0.9	0.300	edge					0.0	0.55	1.55	1.50
0.9										
1.0										
1.1	0.350	edge				0.0	0.05	0.50	1.10	1.10
1.2	0.440	edge				0.01	0.10	0.55	1.00	1.00
1.3	0.480	edge			0.0	0.01	0.15	0.55	0.90	0.85
1.4	0.565	edge			0.01	0.01	0.20	0.52	0.80	0.75
1.5	0.660	edge		0.01	0.01	0.05	0.22	0.52	0.75	0.65
1.6	0.01	0.01	0.01	0.01	0.02	0.07	0.27	0.52	0.65	0.60
1.7	0.01	0.01	0.01	0.01	0.02	0.10	0.30	0.50	0.55	0.50

Table 15. Velocity Field Data (continued)

P_s = 1 psi Control Bias Level 10%

Q_s = 10 CFH Left; Right
1.7 in. oil; 4.7 in. oil

℄	0.1	0.2	0.3	0.4	0.5	0.6	0.7	0.8	0.9	Position
										0.0
(Maximum 7.00 in. oil at right 0.035 inches)										0.1
5.10	3.30	-0.30						0.135	edge	0.1
4.80	2.20	-0.20						0.150	edge	0.2
4.25	1.70	-0.15						0.156	edge	0.3
3.70	1.30	-0.10						0.160	edge	0.4
3.15	1.10	-0.10						0.165	edge	0.5
2.65	0.90	-0.08						0.168	edge	0.6
2.20	0.70	-0.05						0.179	edge	0.7
1.80	0.60	-0.01						0.186	edge	0.8
1.50	0.50	0.0						0.200	edge	0.9
(Maximum 1.70 in. oil at left 0.059 inches)										0.9
										1.0
1.10	0.45	0.01	0.0					0.225	edge	1.1
1.00	0.40	0.03	0.0					0.240	edge	1.2
0.85	0.35	0.05	0.0					0.255	edge	1.3
0.75	0.34	0.10	0.01	0.0				0.330	edge	1.4
0.65	0.32	0.10	0.01	0.01	0.0			0.470	edge	1.5
0.60	0.30	0.11	0.01	0.01	0.01	0.0		0.625	edge	1.6
0.50	0.25	0.12	0.01	0.01	0.01	0.01	0.01	0.750	edge	1.7

Table 16. Velocity Field Data

P_s = 1 psi

Q_s = 10 CFH

Control Bias Level 10%

Left; Right
1.1 in. oil; 5.3 in. oil

Position	0.9	0.8	0.7	0.6	0.5	0.4	0.3	0.2	0.1	℄
0.0										
0.1										
0.1	0.033	edge							-0.45	5.95
0.2	0.094	edge							-0.15	5.20
0.3	0.123	edge							1.00	4.60
0.4	0.152	edge						-0.20	1.05	4.00
0.5	0.189	edge						-0.10	1.40	3.20
0.6	0.215	edge						0.10	1.65	2.60
0.7	0.239	edge						0.25	1.75	2.10
0.8	0.275	edge					-0.05	0.50	1.75	1.70
0.9	0.315	edge				-0.10	0.05	0.70	1.50	1.30
0.9										
1.0										
1.1	0.355	edge				0.0	0.10	0.65	1.25	1.05
1.2	0.410	edge			0.0	0.01	0.15	0.65	1.10	0.90
1.3	0.460	edge			0.0	0.03	0.25	0.65	0.95	0.70
1.4	0.560	edge			0.01	0.05	0.30	0.70	0.90	0.60
1.5	0.680	edge	0.0	0.0.	0.01	0.10	0.38	0.65	0.80	0.60
1.6	0.01	0.01	0.01	0.02	0.03	0.15	0.40	0.65	0.70	0.55
1.7	0.01	0.01	0.01	0.02	0.05	0.20	0.40	0.60	0.63	0.50

Table 16. Velocity Field Data (continued)

P_s = 1 psi Control Bias Level 10%

Q_s = 10 CFH Left ; Right
1.1 in. oil; 5.3 in. oil

¢	0.1	0.2	0.3	0.4	0.5	0.6	0.7	0.8	0.9	Position
										0.0
(Maximum 7.40 in. oil at 0.033 inches)										0.1
5.95	2.35	-0.25						0.129	edge	0.1
5.20	1.75	-0.20						0.141	edge	0.2
4.60	1.25	-0.20						0.146	edge	0.3
4.00	0.90	-0.15						0.146	edge	0.4
3.20	0.70	-0.15						0.147	edge	0.5
2.60	0.55	-0.15						0.159	edge	0.6
2.10	0.45	-0.15						0.160	edge	0.7
1.70	0.35	-0.10						0.165	edge	0.8
1.30	0.30	-0.05						0.171	edge	0.9
(Maximum 1.75 in. oil at left 0.070 inches)										0.9
1.05	0.38	0.01	0.0					0.225	edge	1.1
0.90	0.33	0.01	0.0					0.260	edge	1.2
0.70	0.30	0.02	0.01	0.0				0.350	edge	1.3
0.60	0.30	0.03	0.01	0.01	0.01	0.0		0.510	edge	1.4
0.60	0.28	0.05	0.02	0.01	0.01	0.0		0.550	edge	1.5
0.55	0.25	0.05	0.03	0.02	0.01	0.01		0.620	edge	1.6
0.50	0.25	0.10	0.07	0.04	0.02	0.01		0.810	edge	1.7

Table 17. Control Characteristics

INDIVIDUAL				
Left			Right	
P_c in. Hg	Flow CFH		P_c in. Hg	Flow CFH
9.00	8.0		8.50	8.6
6.00	7.0		6.70	8.0
4.10	6.0		4.90	7.0
2.80	5.0		3.50	6.0
1.95	4.0		2.30	5.0
1.30	3.0		1.60	4.0
.70	2.0		1.00	3.0
.30	1.0		.50	2.0
0.0	0.0		.20	1.0
		TOGETHER		
12.0	9.0		8.8	9.0
9.9	8.0		7.8	8.0
6.9	7.0		4.8	7.0
4.6	6.0		3.50	6.0
3.10	5.0		2.40	5.0
2.10	4.0		1.60	4.0
1.40	3.0		1.00	3.0
.70	2.0		.60	2.0
.30	1.0		.20	1.0
0.0	0.0		0.0	0.0

BIBLIOGRAPHY

1. W. B. Benton, A Fluidic Impact Modulation Test System, Undergraduate Project Report, Georgia Institute of Technology, School of Mechanical Engineering, 1967.

2. Ronald W. McGregor, Parametric Considerations in the Design and Performance of a Fluidic Direct Impact Modulator, Masters Thesis, Georgia Institute of Technology, School of Mechanical Engineering, 1968.

3. P. V. Desai and R. W. McGregor, Parametric Considerations in the Design of a Fluidic Direct Impact Modulator, American Society of Mechanical Engineers Paper, 69-FLCS-38, 1969.

4. M. B. Glauert, "The Wall Jet" Journal of Fluid Mechanics, Volume 1, December 1956, p. 625.

5. W. H. Schwarz and W. P. Cosart, "The Two Dimensional Turbulent Wall-Jet", Journal of Fluid Mechanics, Volume 10, June 1961.

6. A. Sigalla, "Measurements of Skin Friction in a Plane Turbulent Wall Jet", Journal of the Royal Aero. Society, Volume 62, December 1958, p. 873.

7. R. C. Mallonee and S. L. S. Jacoby, Plane, Turbulent Compressible Wall Jet with and without Parallel Free Stream, American Society of Mechanical Engineers Paper 68-FE-40, 1968.

8. H. Schlichting, Boundary-Layer Theory, Sixth Edition, McGraw-Hill, 1968.

9. W. C. Reynolds, W. M. Kays, and S. J. Kline, "Heat Transfer in the Turbulent Incompressible Boundary Layer, I-Constant Wall Temperature", National Aeronautics and Space Administration Memorandum 12-1-58W.

10. B. G. Bjornsen, "The Impact Modulator", Proceedings of the Fluidic Amplification Symposium, Volume II, Harry Diamond Laboratories, 1964.

11. A. H. Shapiro, The Dynamics and Thermodynamics of Compressible Fluid Flow, Ronald Press Company, New York, 1953.

12. R. B. Bird, W. E. Stewart, and E. N. Lightfoot, Transport Phenomena, John Wiley & Sons, Inc., New York, 1960.

13. R. W. Young, "The Jet Beam Deflection Amplifier", Bendix Technical Journal, Vol. 1, No. 4, Winter 1969.

BIBLIOGRPAHY (continued)

14. H. L. Fox and O. L. Wood "Fluid Amplifiers -- The Development of Basic Devices and the Need for Theory", Control Engineering, September 1964, p. 75 ff.